POLITECNICO
MILANO 1863

SCUOLA DI INGEGNERIA INDUSTRIALE
E DELL'INFORMAZIONE

Printability assessment of edible bioinks for cultured meat extrusion-based 3D bioprinting

TESI DI LAUREA MAGISTRALE IN
FOOD ENGINEERING

Author: **Giovanni Zanderigo**

Student ID:	10602107
Advisor:	**Bianca Maria Colosimo**
Co-advisor:	**Filippo Bracco**
Academic Year:	2021-2022

Abstract

Livestock farming is one of the main causes of Green House Gasses emissions, water depletion, and land use. The emerging sector of protein alternatives aims at substituting the consumption of meat from livestock origin. Among the three different types of protein alternatives, cultured meat (CM) is the only one with the potentiality to substitute completely the livestock meat but proposing a product with the same properties. The production of cultured meat follows different procedures, and 3D Bioprinting (3DBP) represents one of the most promising. However, few research is dedicated to the development of this technology, mainly due to the low availability of materials that satisfy the constraints of edibility, biocompatibility, economic feasibility, and printability. This thesis aims at presenting the first empirical printability model that identifies the optimal window of printing parameters considering the model's uncertainty, in order to guide the experimenter according to any objective functions. The focus will be on two edible hydrogels — namely pure alginate 6%, and alginate 6% gelatin 4% — used as bioinks for an extrusion-based 3D bioprinting process for CM. The results of the model aim at opening the doors of scalability and process optimization to this novel technology.

Keywords: Cultured meat, bioprinting, printability assessment, in-situ imaging edible bioink, alginate, gelatin.

Abstract in lingua italiana

L'allevamento di bestiame è una delle principali cause delle emissioni di gas serra, dell'impoverimento delle risorse idriche e dello sfruttamento del suolo. Il settore emergente delle alternative proteiche mira a sostituire il consumo di carne di origine animale. Tra i tre diversi tipi di alternative proteiche, la carne coltivata è l'unica con la potenzialità di sostituire completamente la carne di origine animale, proponendo un prodotto con le stesse proprietà. La produzione di carne coltivata segue diverse procedure, e il 3D Bioprinting rappresenta una delle più promettenti. Tuttavia, poche ricerche sono dedicate allo sviluppo di questa tecnologia, soprattutto a causa della scarsa disponibilità di materiali che soddisfino i vincoli di commestibilità, biocompatibilità, fattibilità economica e stampabilità. Questa tesi mira a presentare il primo modello empirico di stampabilità che identifica la finestra ottimale dei parametri di stampa tenendo conto dell'incertezza del modello, al fine di guidare lo sperimentatore in base a qualsiasi funzione obiettivo. L'attenzione si concentra su due idrogel commestibili — alginato puro al 6% e alginato al 6% e gelatina al 4% — utilizzati come bioink per un processo di bioprinting 3D ad estrusione per carne coltivata. I risultati del modello mirano ad aprire le porte della scalabilità e dell'ottimizzazione del processo a questa nuova tecnologia.

Parole chiave: Carne coltivata, bioprinting, valutazione di stampabilità, raccolta immagini in-situ, bioink commestibili, alginato, gelatina.

Summary

Introduction

This introduction aims at exploring the background of the thesis, in order to understand the processes and technologies involved in the Cultured Meat industry, the related issues, and the opportunities that characterize it. The structure of this introduction will follow a cascade approach, starting from the generic point of view of the topic, that will later focus more and more up to the topic of the thesis.

This disclosure starts from the cultured meat framework, in which are proposed the drawbacks of the traditional livestock farming, and the novel interest of the market towards protein alternatives driven by the environmental concern. From that, the subject of the introduction will focus on the cultured meat as protein alternative, and on its production procedures. Eventually the introduction will finish on the exploration of the 3D bioprinting techniques, and on the materials involved for this specific process.

Cultured meat framework

A livestock meat Life Cycle Assessment

Proteins — large macromolecules composed by amino acid — are the building block of our metabolism. The digestion breaks them into amino acids, and they later achieve vital functions (Gaillac & Marbach, 2021). Thus, proteins are

fundamental in our diets: the globally established dietary reference intake for a person in good health — not involved in any major sport training — is about 0.8 g of proteins per kg of body weight per day (Gaillac & Marbach, 2021).

To this day meat is still the major source of proteins for human diet. So, the demand of livestock by the food industry is steadily increasing with the growth of the world population and the higher disposable income. But such a huge and uncontrolled production of meat and meat based food brings many repercussions on the environment.

The world food supply chain produces 13,7 billion metric tons of carbon dioxide equivalents (CO_2 eq.) that represents the 26% of the total anthropogenic green-house gas (GHG) emissions (Poore & Nemecek, 2018; Gaillac & Marbach, 2021). As the livestock farming is worth more than half of the emissions produced from all the food supply chains, it is responsible for at least the 14% of the total world emissions (Gaillac & Marbach, 2021; Springmann et al., 2016).

The GHG emission in livestock farming process depends on many factors such as the methane released by the cows, the farm machineries and engines exhausts, the emissions connected with the crops growth to feed the livestock, together with the pollution related to the transport, processing, packaging and retailing systems.

Alongside the GHG emissions, we have also to consider the impact of the livestock supply chain on other relevant environmental aspects.

First of all, livestock intense farming plays a key role in the land usage. According to FAO, the 70% of all agricultural soil and the 30% of earth's land surface are directly or indirectly related with the livestock breeding (Ilea, 2008). Beef production is the cause of deforestation and negative practices such as uncontrolled burning of fields to increase the available meadows in cheap and

quick ways. The 97% of the land involved in the production of beef is used for the feed crop cultivation (Asem-Hiablie et al., 2018). Moreover, the fields where the animals live get poisoned by the excretion making the soil unusable to any further agricultural growing.

According to data coming from US farming, 5.126 litres of water are consumed in the whole production process per each kg of boneless, edible beef (Asem-Hiablie et al., 2018). This huge quantity of water — as happens for the land — is mostly absorbed (around the 98%) by the irrigation of the crops to produce the animal feed.

Another important impact on the environment, is caused by the chemicals introduced in the livestock intense farming. Due to the high density of animals in the farms, the spread of diseases is extremely easy and uncontrollable; thus, in order to maintain high production standards and minimize losses, the food industry started to give antibiotics to the animals in a massive way. If this practice is particularly strong in poultry breeding, it is nevertheless applied in all the different livestock farming industries. Furthermore, the massive use of antibiotics makes the livestock a reservoir of antibiotic-resistant organisms that switch to man through the ingestion of meat; and this has been evaluated as the cause of 33,000 deaths per year in Europe (European Commission, 2021; Ferroni et al., 2022).

The medical research also proved that high protein intake from livestock is related with the onset of some diseases. In particular way, some age-related diseases (like diabetes, cardiovascular diseases, cancers) are connected to the intake of 0.8 g/kg/day proteins of animal origin. This is especially true for red meat and even more for processed meat (Gaillac & Marbach, 2021).

Despite the fact that all these elements — connected with the growth of the demand — seem to push to a worse and worse scenario, in the last period we can observe an important inversion to the 'no rules' production trends. Along with a different feeling towards the animal husbandry conditions — thanks to the opinion struggles of the animalist organizations — it is growing a much higher attention about the dangers for the consumers' health due to uncontrolled presence of chemicals in the meat, and a wider awareness against the land waste and the soil pollution.

In this perspective, has emerged the necessity to switch part of animal-based products — which, as mentioned above, are responsible for the 14% of GHG emissions — in alternative food supplies. If a strong Governments' will and the development of the research will push in this direction, a reduction within 2030 of the 11% of currently emissions seems a target affordable (Morach et al., 2022).

The study of protein alternatives is thus an urgency and plays a key role for the industrial food research.

The role of protein alternatives

The term protein alternative refers not only to the meat alternatives, such as beef, pork, poultry, fish and other types of livestock, but also includes eggs, milk, fresh dairy and cheese.

According to the reports published by BCG (Boston Consulting Group) and Blue Horizon in 2021, Food for Thought, the protein alternatives represent the 2% of the globally consumed proteins in 2020. However, due to the increasing interest towards these kind of alternative food, it is forecasted a growth at least to the 11% by 2035 (Figure 1) (Witte et al., 2021).

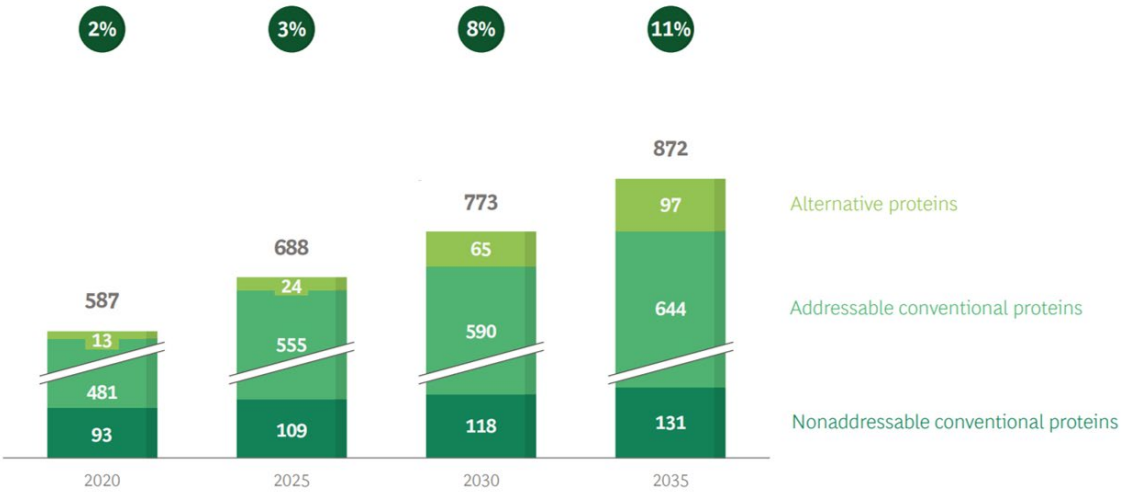

Figure 1: Global consumption of protein products (Source: US Department of Agriculture; Euromonitor; UBS; ING; Good Food Institute; expert interviews; Blue Horizon and BCG).

This forecast is based on the effect played by four dominos, even considering the most realistic case in which only the first two dominos get fully triggered.

The first domino is already triggered and consists in the public concern for the climate and sustainability. In fact, most consumers are going to reduce the amount of animal proteins in their diets, moved by their commitment to sustainability.

The second domino is the refinement and scaling of the existing technologies. This scenario is triggered by the increasing of the demand, and consequently by the interest of the investors to develop protein alternative food. The final goal of this step is to achieve a product whose price is equal to the conventional meat price and with a texture and a taste that closely match it.

The forecast points out that the full development of these two first dominos is sufficient to achieve a consumption of 11% of global proteins coming from alternative sources.

In this way, the activation of the last two dominos will have the effect of giving a significant acceleration to the phenomenon.

The first of these further scenarios consists in the possibility that the incumbent food companies, along with the startups supported by public and private institution investments, achieve a better production efficiency and obtain a superior taste and texture in their products. This will generate a even more strong interest for this kind of foodstuffs, achieving the 16% of the overall consumption of proteins by alternative sources by 2035 (Figure 2).

The fourth domino will realize when regulations come into play. If there will be a push by Regulation institutions in facilitating farmers and industries to shift to alternative protein production, this market will achieve a 22% share of overall protein consumption by 2035 (Figure 2) (Witte et al., 2021).

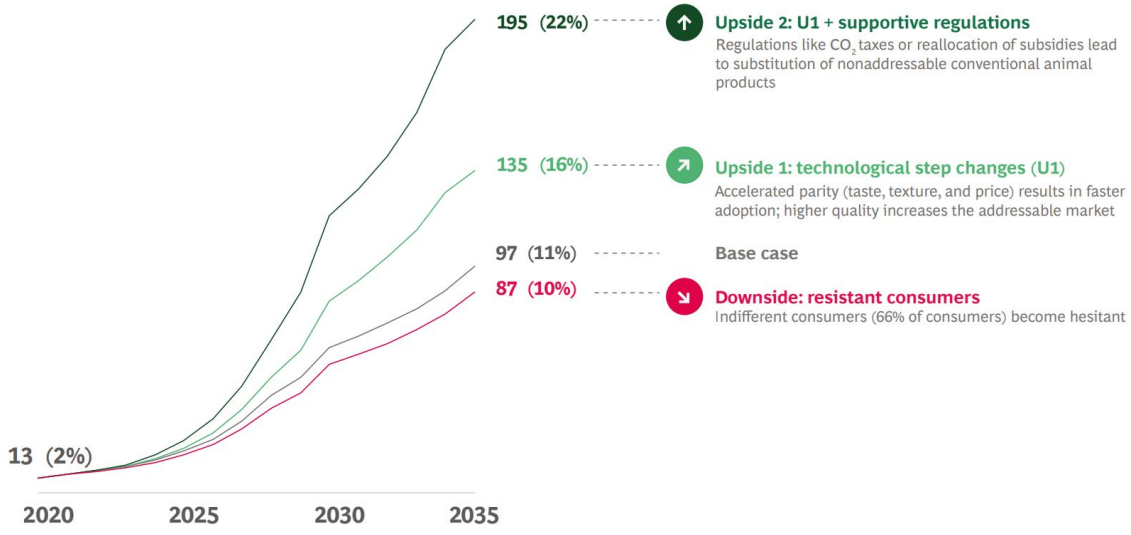

Figure 2: Million metric tons and % of penetration of alternative proteins (Source: Blue Horizon and BCG analysis).

Types of protein alternatives

Protein alternatives can be divided into three families:

- Plant-based
- Microorganism-based
- Animal cell-based

Plant-based

Plant-based alternative proteins consist in protein flours - typically derived from soybeans and yellow peas - compounded with additives to form a product that resembles the taste and the texture of meat. Among the protein alternatives they represent the most consumed product, due to their high commercialization. This depends not only on the availability of the raw material and quite simple industrial processes, but also on their wide possibility to comply with regulations and rules. In fact, microorganism-based and animal cell-based alternatives still need to be regulated in most of the countries and, to this day, cannot be easily commercialized.

Even if this kind of products are the most common, they haven't overcome the problems of scalability yet. The main issues are related to the crops optimization, protein extraction, cost and complexity of additives and texturing compound. This makes the production more costly when compared to livestock farming, at a level that, at the moment, the cost of the final product is almost the double of conventional meat. However, due to the high investment forced by the increased consumption, the cost of these protein alternative is forecasted to reach the cost of conventional animal-based meat by 2023 (Figure 3) (Witte et al., 2021).

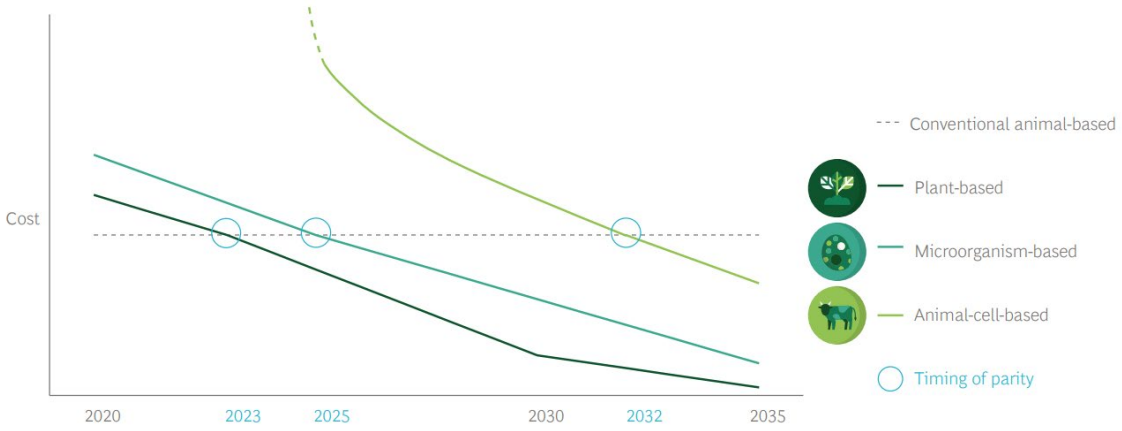

Figure 3: Relative timing of cost parity for alternative proteins with realistic taste and texture (Source: Expert interviews; industry reports; Blue Horizon and BCG analysis).

In the subsequent report of 2022 by BCG and Blue Horizon, these forecasts were reanalysed with new data, and confirmed to be in line with the predicted timing of parity (Appendix 2) (Morach et al., 2022).

In the plant-based industry we can find famous brands - such as Beyond Meat or Impossible Food, working in this sector from a long time - which have achieved high levels of revenues yet. Along with these established brands, quite a lot of new companies are entering the market through the use of new technologies, such as Redefine Meat that is testing an innovative use of 3D printing to get a better quality to the final product's shape and texture.

Microorganism-based

Microorganism-based protein alternatives are the second category entering the market. These alternatives are produced using bacteria, yeasts, single-celled algae, or fungi that are flavored and texturized into edible products.

In order to produce this kind of proteins, two processes can be adopted:

- precision fermentation, where microorganisms are grown in a liquid suspension culture to produce a specific protein;

- filamentous fungi, that are grown in a solid state culture (common for the production of meat alternative).

These alternatives ranked second in the race to reach the costs equality with conventional animal meat, and they are forecasted to achieve it in 2025 (Figure 3). At the moment there are still many challenges to face in order to reach this target, like the metabolic efficiency of microorganisms, the high costs of feedstocks and additives, and the efficiency of protein extraction. These difficulties are resumed in a statement of the Quorn's CEO, Kevin Brennan: "*it took six weeks to find the right microorganism, and 20 years to get the process to work reliably at scale*" (Witte et al., 2021). Quorn is the leading company of this market, which has been selling meat replacement products since 1985.

Animal cell-based

The third category of protein alternative are the animal cell-based alternatives. These alternatives include the so-called "*cultured meat*", or "*cultivated meat*", a product derived from the cultivation of animal cells taken from a living animal and then grown in a nutrient-rich medium to generate thousands of kilograms of flesh of the donor species' cell.

Compared to the other protein alternatives, the cultured meat is the farthest from reaching equal costs with conventional meat, due to the complexity of the process (see next chapter) and to a difficult compliance of these products to the current regulations together with the slow process to adjust the laws on the subject. In fact Institutions started to give regulatory support only in the last years, with an accelerating trend (Figure 4) involving also plant-based and microorganism-based protein alternatives (Morach et al., 2022).

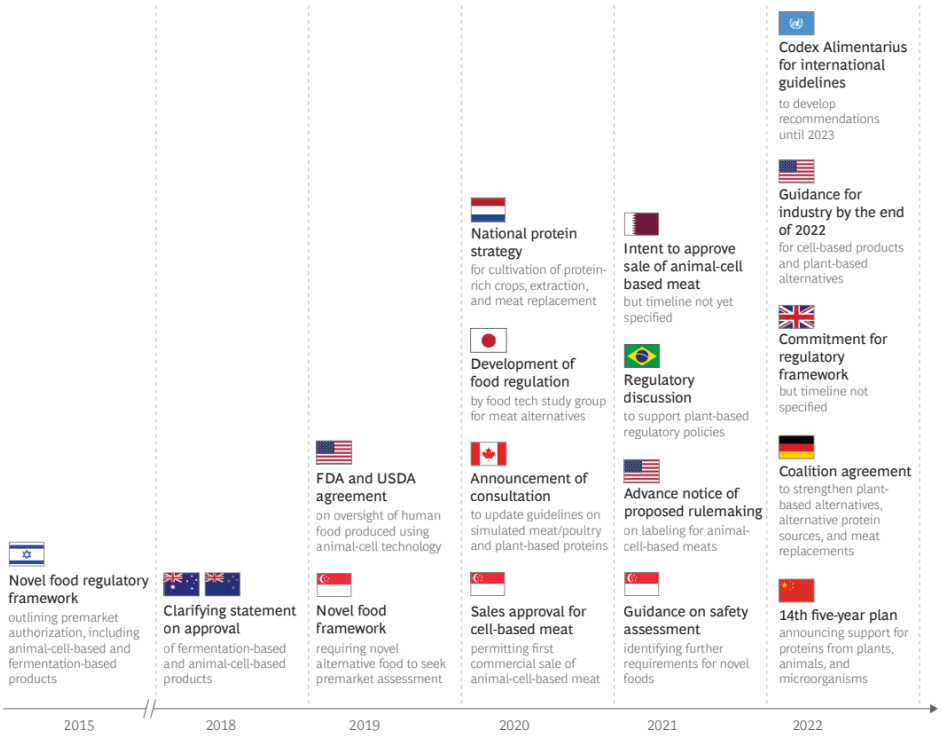

Figure 4: Regulatory Support for Alternative Proteins (Source: The Good Food Institute; FAIRR; official government regulations; Blue Horizon and BCG analysis).

For these reasons, the goal of price parity is forecasted to be reached in 2032 (Figure 3).

Concerning the process, experts claim that to reach the parity first of all is necessary to increase its metabolic efficiency, as well as overcoming the cost of the nutrient-reach media and adopting key non-animal materials for the cell growth (Witte et al., 2021).

However, this alternative is the only one having the potential to completely replace the conventional meat: as stated by many companies in their manifesto, cultured meat is not '*like meat*', but it '*is meat*'. Moreover, on environmental side, the differences between cultured meat and conventional meat are many, and radical.

Due to the novelty of the process and its distance from the scales of the real market, an environmental Life Cycle Assessment study about cultured meat —

in which the amount of kg of CO_2 equivalent is stated and compared with conventional meat — is not available yet. However, just looking at the process, many of its environmental impacts are clearly and immediately different from the conventional livestock meat.

The water and the land consumption are drastically reduced since there is no need to grow the feed crops. The production is in fact related only to facilities where the cells are grown in bioreactors. This process consumes an amount of water comparable to the quantity drunk during the livestock lifetime, that means only the 2% of the overall water usage in the conventional meat supply chain.

Cultured meat is, by definition, a product without antibiotics since there is no need of them. In fact, only animal cells are selected from the animal, with no contaminations from other micro-organisms. These cells stay in a completely aseptic environment during all the culture phases, leading to a sterile product.

In the case of cultured fish, it must be also considered the great advantage of shifting the production sites from the sea to the land. In fact, the traditional fish farms impact heavily on the biodiversity of the seas because they create micro zones where single species are concentrated. Moreover, this concentration brings to an intense fishing activity that amplifies the same phenomenon.

Production procedure of cultured meat

As mentioned in the previous chapter, cultured meat follows a precise — although full of complexities — workflow. The process was born as a deviation from Tissue Engineering (TE) and Regenerative Medicine, a field of the Biomedical Engineering that aims at restoring, improving or replacing biological tissues, involving human cells that remain viable during all the process.

The traditional TE for biomedical applications aims at producing functional biological tissues, that can be integrated into patients and play a vital function. The tissue has to be biocompatible with the patient, but the edibility is not a concern. In the other hand, TE for CM applications starts from animal cells, and aims at producing biological tissues that doesn't have to be functional but must be mandatorily edible and nutritive.

This process can be summarized in four main steps: cells harvesting, proliferation, generation of the 3D tissue, and cell differentiation (Figure 5).

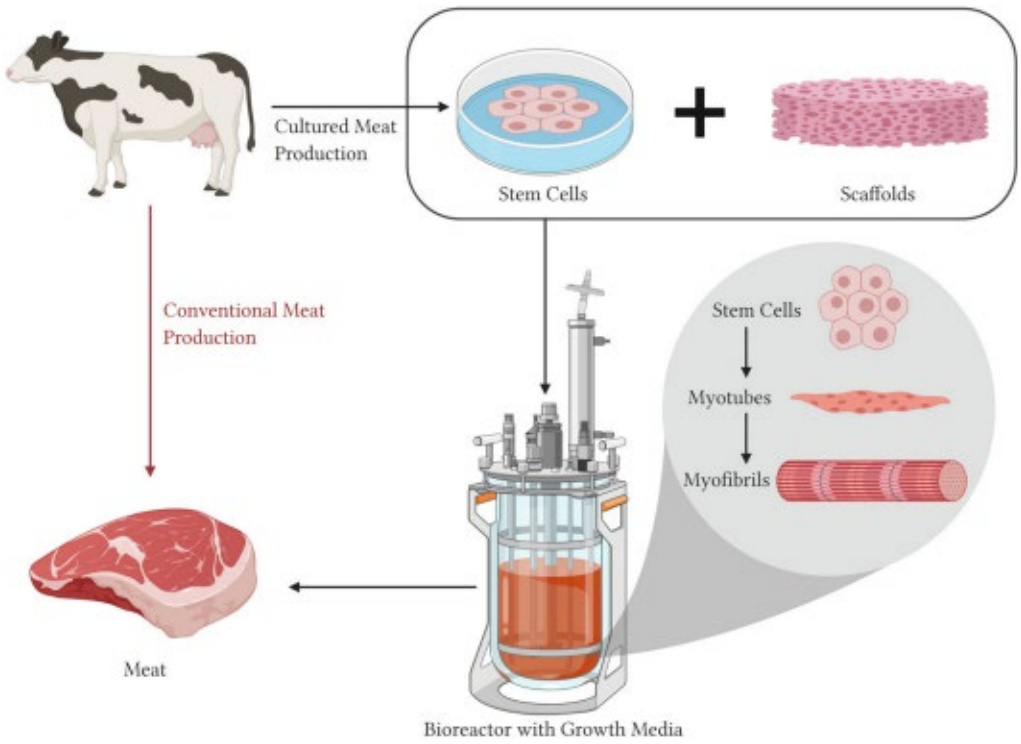

Figure 5: Cultured meat production and conventional meat production processes (Source: BioRender.com, H. K. Handral et al.).

Cells harvesting

The process starts with the cell harvesting. The cells are gathered in three main different ways (Lanzoni et al., 2022):

- multipotent muscular cells taken from a living animal;

- pluripotent embryonic stem cells induced in the formation of muscle cells;
- immortal cells lines.

The most common is the first way, where Myosatellite cells are directly obtained by a living animal, without harming it through a painless sampling. In this phase the donor animal is sedated, and a small portion of its tissue is taken. The tissue sample is very small, typically 0,5 grams, as large as a corn grain, but contains the quantity of cells necessary to start a proliferation activity capable of generating the organic material to produce almost 100.000 hamburgers.

Cell proliferation

The next step in the process is the cells proliferation. This step aims only at duplicating repetitively the cells up to a number that satisfy the requirement of production.

In laboratory scale, the cells are grown in a bidimensional plate where they are well anchored and can therefore grow. For the industrial applications are instead used bioreactors - usually tank reactors where cells are suspended in a nutrient-rich proliferation media and are allowed to proliferate - in order to scale up the production.

Three techniques are commonly used to address the proliferation: culture in aggregates, culture on microcarriers and culture in packed bed reactors (Figure 6) (Bodiou et al., 2020).

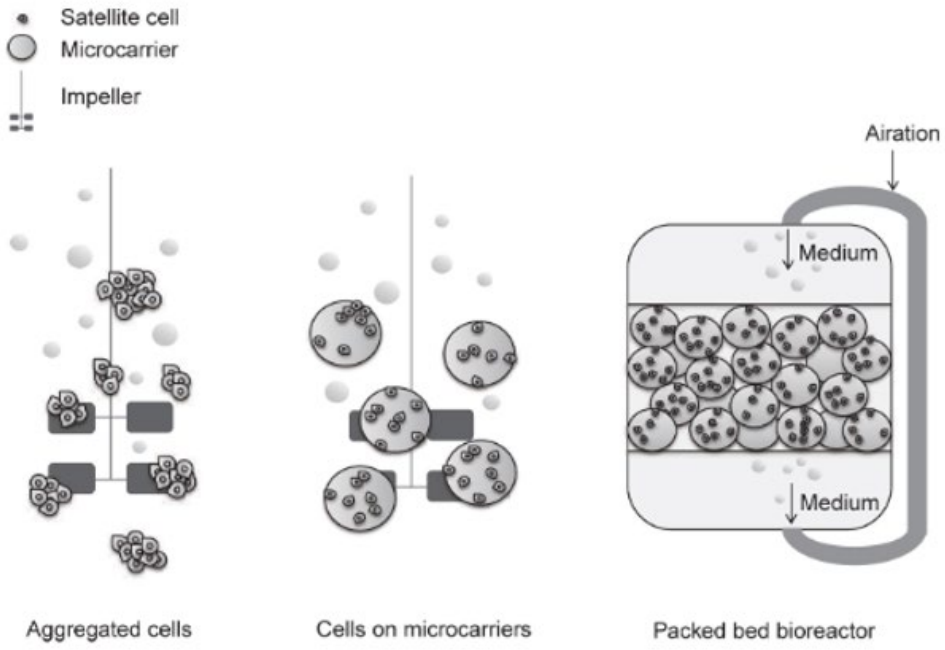

Figure 6: Overview of the three possible scaling-up systems for cultured meat (Source: modified from Moritz et al., 2015).

The first refers to the formation of clumps of cells that grow in 3D and serve as anchors for their neighbors. They grow suspended in the proliferation media in a stirred tank reactor (Moritz et al., 2015). Although this technique proves to reach high cell densities in the bioreactor, the little control in clump size generates large structures with nutrients and O_2 gradients that cause necrotic cores (Bodiou et al., 2020).

What gained interest for its efficiency is the use of microcarriers. Microcarriers are small spheres of biomaterial where cells can adhere and grow. They substitute the cellular core of the 3D aggregates with a biomaterial, that will provide a solid anchor for the cells in order to grow in a 2D surface. The use of microcarriers avoids the necrotic core of the 3D aggregates but keeping the clustered structure of the aggregates. Microcarriers that offer a large surface/volume ratio are the most promising candidates for high efficiency scalability (Bodiou et al., 2020).

The second method for scalability, which is the one that gained most interest, is the adoption of microcarriers in stirred tank reactors, similar to the one used for the 3D aggregate. They are typically 100-200 microns in diameter, made in materials that can be either edible, non-edible but soluble (sacrificial material) or non-edible and non-soluble, that has to be subsequently separated from cell clusters.

The third method consists of Packed Bed Bioreactors (PBR) where cells are immobilized in a solid bed of microcarriers. In this case the reactor is stationary, and the media flows through the microcarriers (Moritz et al., 2015).

The proliferation step represents a challenge for the process because the proliferation media used are very costly, and the more traditional ones are derived from animal fetus that makes them costly and with low reliability (every batch may differ from the others). Therefore, there is much research in the development of new alternatives with animal free ingredients and with a cheap production cost.

Three-dimensional tissue fabrication

Once that the desired number of cells is reached, the cells have to be distributed in a 3D structure. The final tissue fabrication can be accomplished only if the cells are provided with the correct environment in which they can adhere, proliferate and differentiate (Lanzoni et al., 2022). Moreover - unlike the laboratory conditions where cells are grown typically in 2D plate cultures - the new tissue has to proliferate in a 3D pattern and, therefore, the required environment must be a three-dimensional solid structure with voids where cells can solidly adhere.

Scaffolding

The answer to this necessity is the scaffold: a preformed 3D structure of biomaterial, realized with the desired porosity or texture able to guarantee the three-dimensional proliferation and differentiation of the seeded cells. Scaffolds provide physical and biochemical cues for the cells to adhere, proliferate and differentiate into the necessary cell types, allowing spatial heterogeneity in the final product that will resemble the natural meat structure and texture (Seah et al., 2021).

Scaffolds can be obtained by the decellularization of tissue/organs , an expensive methodology with lack of applications, or can be crafted. The crafting can be achieved through non-AM techniques, like electrospinning, solvent casting, thermal-induced phase separation, gas foaming and freeze-drying, or by AM techniques like stereolithography, selective laser sintering, fused deposition modeling and solvent-based extrusion preforming (Figure 7) (Seah et al., 2021).

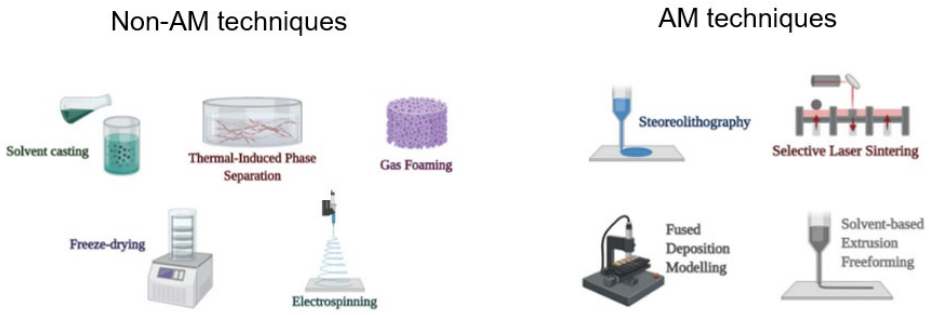

Figure 7: Scaffold crafting techniques (Source: modified from J. Si Han Seah et al.).

The process of producing scaffolds through AM in no longer called '*3D Bioprinting*' (as for the case of Biofabrication), but instead '*3D Printing*', because no cells are involved, but only the 3D empty scaffold is produced.

Each technique for scaffold crafting will generate scaffolds with different architectures, which will eventually interact with cells in diverse ways (Figure 8).

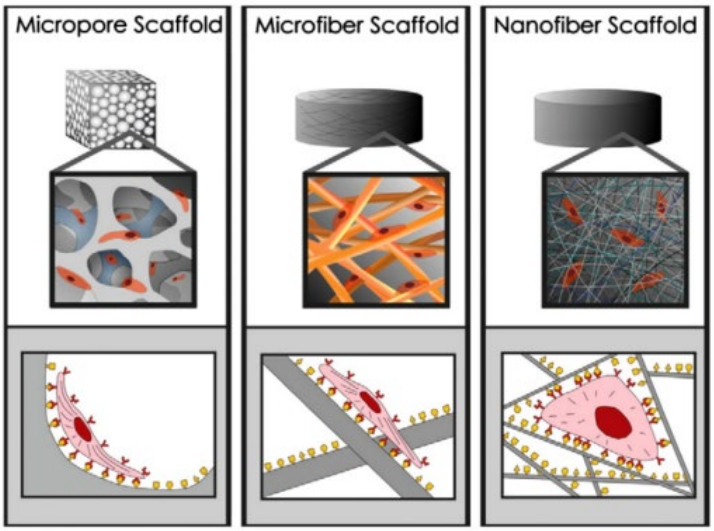

Figure 8: Cells interaction with different scaffold architectures (Source: Zhu & Che, 2013).

Once that the scaffold is crafted, the process of tissue fabrication proceeds by seeding the cells in the preformed scaffolds and maturing the tissue in nutrient-rich environment.

Scaffolding (the practice of tissue fabrication though scaffolds) however has a limit represented by the diffusion of nutrients. Scaffolds have a critical thickness, in the order of the microns depending on the different materials and shapes, over which the cell and nutrient diffusion would not be enough to reach the core of the scaffold. In fact, it is reported that cells do not trespass a critical diffusion thickness of 500 μm (Sachlos et al., 2003). This means that to have a desirable thickness — in the order of the millimeters or centimeters — multiple scaffolds must be stacked. This creates a limiting factor for the cultured meat production, due to the low scalability of this practice.

Biofabrication

A recent and promising technology for the 3D tissue fabrication is the Biofabrication: a technology based on Additive Manufacturing (AM) where cells embedded in a bioink are directly printed in the final 3D structure. As for the scaffolds, the bioink must have a reticular micro-structure with voids where the cells can adhere. Since the cells are directly deposited with the bioink, the seeding step can be avoided permitting the generation of a thicker structure, if provided with the adequate vascular system. This key aspect is one of the most promising advantages of this kind of approach, since the 3D tissue fabrication will be achieved only in one step, with large margin of scalability.

Biofabrication does not necessarily aims at generating complex tissue, but also unlocks the hybrid opportunities where cell-laden bioinks are integrated in scaffolds or external structures that promote cell growth and differentiation (Vijayavenkataraman et al., 2018).

Biofabrication starts with the generation of the 3D model that has to be printed. Once defined the shape, the different combinations of cells and bioinks are chosen and formed by mixing the bioink with a solution of salts and suspended cells. Cell-laden bioinks are loaded in cartridges and installed in the bioprinter. In Biofabrication applications there are five main AM techniques: extrusion, inkjet, laser-assisted, stereolithography and two-photon (Figure 9) (Santoni et al., 2022).

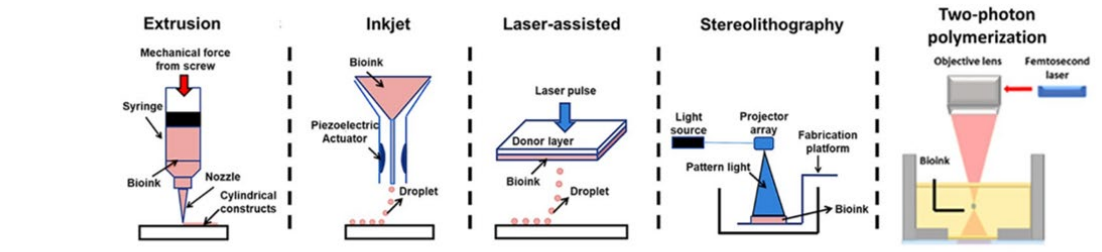

	Extrusion	Inkjet	Laser-assisted	Stereolithography	Two-photon polymerization
Speed	Slow	Fast	Medium	Fast	Very fast
Cost	Moderate	Low	High	Low	Very High
Cell viability	85-95%	80-95%	<85%	>90%	>80%
Cell density	High	Low	Medium	Medium	Medium
Resolution	100 - 500 µm	100 - 500 µm	20 -100 µm	20 -100 µm	0,1 - 10 µm
Viscosity	6-30 × 10^7 mPa·s	<10 mPa·s	1-300 mPa·s	No limitation	No limitation
Applications	Tissue models for basic cell research, drug testing and	Supplementary to other technologies	Precision cell deposition	Scaffolds and complex structures with channels	Vascularized and high precision models

Figure 9: Different 3D Bioprinting techniques and their relative characteristics (Source: Santoni et al., 2022).

Due to the features of the process, biofabrication introduces many advantages. Cells density and deposition pattern can be controlled during the deposition. Additionally, the AM nature of the process guarantees additional advantages: it has higher scalability, it is complex free, and it permits the simultaneous processing with different configurations of materials and cells (K. Handral et al., 2020). This unlocks an incredible number of configurations in textures, tastes, and combinations of different cells (such as muscle and fat cells).

Cell differentiation

The last step of the cultivation process is the cells differentiation and proliferation in bioreactors. The aim of this step is to completely fill the scaffold or bioink, until cells will occupy all its voids, forming a dense tissue composed of muscular fibers.

As mentioned, the cells involved are usually Myosatellite, multipotent muscle stem cells that have the potential to differentiate into Myoblasts, the building block of Myotubes. Myotubes, lastly, have the potential to merge and create the

structures of Myofibers, which compose the macrostructure of muscle fibers (Figure 10) (Zammit et al., 2006).

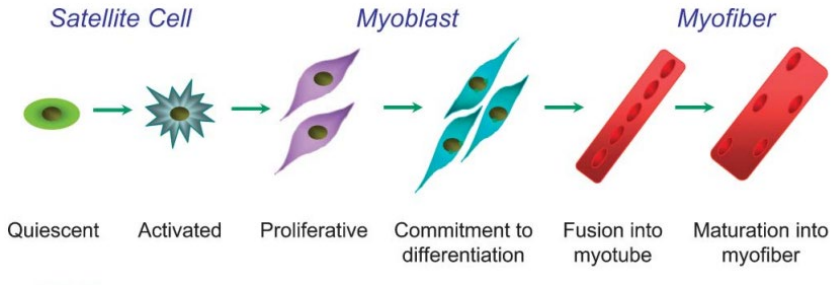

Figure 10: Schematic of satellite cell myogenesis (Source: Zammit et al., 2006).

In order to trigger this pathway, the 3D tissues are put in bioreactors. In this environment, the cells are stimulated by specific chemicals present in the differentiation media (different from the proliferation media), that triggers their differentiation. In addition, cells can also be exposed to mechanical or electro-chemical stimulation to achieve a complete myofiber formation and alignment.

Bioreactors are closed environments, with automated circulation system. They are essential to provide the same amount of growth media to all the 3D tissue that are contained within it, and to guarantee a constant intake of fresh media. It is essential that the growth media is kept fresh, otherwise the metabolic wastes produced by the cells during their differentiation - which can be either degraded scaffolds or secreted metabolites from the bioreactor - will saturate the media and intoxicate the cells.

3D Bioprinting for cultured meat

AM finds applications both in scaffolding and biofabrication processes. However, bioprinting with cell-laden bioinks is the characteristic that distinguishes biofabrication.

Due to the presence of cells in the bioink, not all the traditional AM processes can be adapted to bioprinting. Those that can be adapted, instead, have different advantages and disadvantages that differentiate their applications.

Extrusion Based

Among the 3DBP approaches the most common are the extrusion-based. This method has high versatility thanks to the easy availability of materials, and the equipment needed is relatively inexpensive and simple. The bioprinters are often produced internally by laboratories guaranteeing the highest control on the equipment; however many entry-level machines are easily found on the market, provided by specialized companies.

In extrusion based, the cell-laden bioink reserved in a cartridge is extruded thorough a nozzle of pre-defined diameter. The driving force is provided by an extruder operating on the back of the syringe-like cartridge. The process can be either at constant pressure — when the extruder is a compressor that applies a constant pressure to the cartridge — or at constant flow rate of bioink - when the extruder is a piston or a screwed motor that pushes the back of the cartridge with a constant velocity - (Appendix 3). The deposition of material is controlled by the print-head, which moves along the x and y axis, while the print bed is able to move along the z axis (Figure 11).

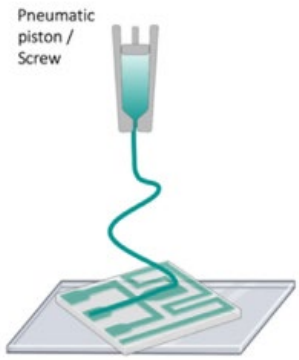

Figure 11: Schematic representation of extrusion-based bioprinting (Source: Rothbauer et al., 2022).

The bioinks used in this process must guarantee specific rheological properties. In particular, the bioink has to be viscous before extrusion, in order to be easily extruded, and solid after extrusion, in order to keep its shape. In order to achieve this dual rheology, bioinks are kept viscous during the extrusion process, and undergo solidification after the deposition (typically through chemical or UV cross-linking). This permits to extrude with low pressures that do not damage the cells, guaranteeing later that the printed shape will last during all the subsequent processes of culturing.

The high viscosity of the bioinks used in this process unlocks the possibility to bioprint with high cellular density. This process is typically slow and has the final quality of the object limited by the dimension of the nozzle, because the printed features can't be smaller than the nozzle diameter in fact.

Inkjet

Another widespread technology in the field of 3DBP is the inkjet technique. As for extrusion-based, the material range is large, but the equipment complexity is higher with respect to extrusion-based.

In this case the cell-laden bioink is not extruded in a continuous stream, but in droplets. The droplets are formed by an actuator, that can be thermal or piezo-electric. It aims at pushing the bioink through the nozzle and form the droplet of desired dimension. Moreover, the droplets can be supplied on the substrate through three approach: in a continuous inkjet bioprinting, with an electro hydrodynamic jet bioprinting, and through a drop-on-demand inkjet bioprinting (Derakhshanfar et al., 2018) (Appendix 4). The latter approach with thermal or piezoelectric actuators is at the moment the most common approach of inkjet 3DBP. As for extrusion-based bioprinters, the print-head must be capable of scanning along the x and y axis, while the print bed moves along the z axis (Figure 12).

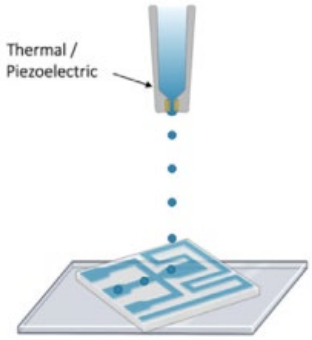

Figure 12: Schematic representation of inkjet bioprinting (Source: Rothbauer et al., 2022).

Bioinks used for inkjet must have a desired rheology in order to be used in this process. Their viscosity in fact must be in such interval that is low enough to be extruded in the form of a droplet, but high enough to remain in shape before the curing (the solidification step). However, their viscosity is generally way lower than the bioinks used for extrusion-based 3DBP, usually lower than 10 mPa s (Derakhshanfar et al., 2018). This also impacts the cell density that can be deposited with this process, that results lower than extrusion-based.

As for the extrusion-based bioprinting, the bioink has to be viscous during deposition, and after being printed is cured either chemically or by UV light.

The process is faster and more precise than extrusion-based bioprinting. In fact, droplet deposition and dimension can achieve the printing of small features. Nevertheless the process is characterized by the issue of clogging: the bioink occasionally dries or cures on the nozzle, causing its occlusion and the incapacity of depositing further droplets.

Laser-assisted

The laser-assisted is a technology presented for the first time 30 years ago. Due to the necessity of a system to create and to focus a laser beam, the equipment is quite complex; this, along with a low material availability, make such a technology of low interest today.

The process is based on the laser-induced transfer principle: it uses a pulsed laser beam that acts, through a focusing system, on a ribbon composed by a donor transport support material covered by a laser-energy-absorbing substrate and a biological material layer. The focused laser pulses on the absorbing layer generates high-pressure bubbles that propel the material against a collector substrate facing the ribbon (Figure 13) (Lanzoni et al., 2022).

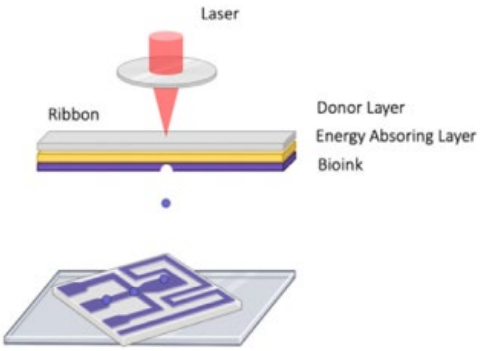

Figure 13: Schematic of Laser-assisted Bioprinting (LAB) (Source: Rothbauer et al., 2022).

Starting from the laser incident side, the ribbon is composed by a donor slide, succeeded by a laser absorbing layer and a bioink film on the opposite side. When the laser impacts the surface of the ribbon it causes the evaporation of a precise spot of biomaterial. The dimension of this spot is a function of the laser intensity, accounting that 99% of the light passes the transparent biomaterial and does not influence the process (Derakhshanfar et al., 2018). The amount of light has to remain under a certain limit that, if overcame, can irreversibly damage the cells.

Despite its complexity, LAB bioprinters have a high resolution without using nozzles. This avoids many issues related to nozzles — first of all the clogging — and is able to deposit bioinks in solid and liquid form.

However, the presence of metallic residues in the final product is a major safety concern for food systems, restricting the use of LAB for the commercial production of CM (Levi et al., 2022).

Stereolithography

Stereolithography is the first polymer AM technique ever invented, that later got adapted to biopolymers. The equipment is composed of a vat, where the liquid

bioink is stored, a UV light source, and a focusing and scanning system for the UV beam.

This process is based on the photo-polymerization of the bioink: in the vat the photo-curable material gets stimulated by a spot of UV light that scans the surface of the material along the x and y axis. The UV will trigger the polymerization, cross-linking a portion of the bioink. When the UV light spot has scanned the layer, the bed supporting the cured structure moves by a layer along the z axis (Figure 14).

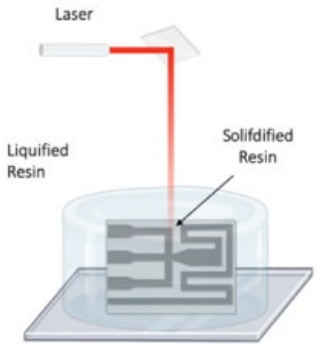

Figure 14: Schematic of Stereolithography (STL) bioprinting (Source: Rothbauer et al., 2022).

As mentioned, for this process the bioinks must have an important feature: they have to be photo curable. This feature is a constraint that limits the range of biomaterials for this technology. Photo curing can be also a cause of mortality for cells, making the UV light intensity a delicate parameter to manipulate during processing. Additionally, among the different 3DBP techniques, this is the only one that cannot operate multi-material in the same processing stage.

Despite these drawbacks, the STL bioprinting has the highest geometrical accuracy among the other AM techniques, is nozzle free, and can print extraordinarily complex shapes.

Two-photons

Two photon is a particular type of Stereolithography. Nevertheless, it is considered different from STL since the UV light beam is substituted by two converging photon sources.

In this process the polymerization is triggered only when the material is stimulated by two photons simultaneously. In this way, adjusting the focus, the two photon source it is possible to identify a single spot in the vat that will get cured. This approach enables to reach outstanding feature accuracy - in the order of the nanometer - together with the capacity of scanning in the vat along the x, y and z axis, without having a moving bed (Figure 15).

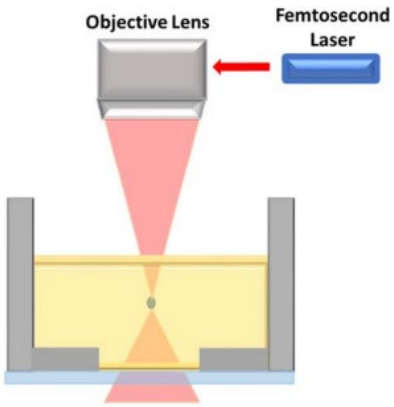

Figure 15: Schematic of Two-Photon bioprinting (Source: Ng et al., 2020).

As for STL bioprinting, the bioink must be photo curable. Again, this limits the range of usable material, but unlocks the unique precision of this technique. Furthermore, it is a nozzle-free technology and has very fast scanning speed. However, due to the high complexity of the equipment, it is limited to laboratory-scale productions.

Monitoring in 3D bioprinting

Traditional AM technologies have been highly successful, especially in applications in which high shape complexity is involved. Most of the time the technology is used in fields, such as biomedical or aerospace, where tolerance to defects is critically low. For this reason, the quality of AM technologies is more and more pushed by intelligent monitoring systems at a different level of investigation both with in-situ and ex-situ techniques (Colosimo et al., 2018; Everton et al., 2016).

The layer-by-layer mechanism of AM allows to have a detailed view of the printed object, permitting to monitor the process at a very high detail level. This can be for example the image collection during the fabrication of each layer up to the control of the nozzle temperature during the process (Bugatti & Colosimo, 2022). According to Grasso and Colosimo, AM process monitoring will be one of the key features of the upcoming generation of 3D printers.

In order to produce a reliable monitoring system able to detect defects, correlation between observable features and final defects must be carefully evaluated. Moreover, in-process data analytics allow to gather large amount of data quickly to detect the real time defects and process errors. The adaptation of the process parameters based on in situ measured quantities and the implementation of closed-loop repairing actions can then imply the elimination of errors during the processing (Grasso & Colosimo, 2017).

Monitoring the geometrical fidelity of the printed objects with in-situ image analysis unlock the possibility to make real-time adjustments of the process parameters that are correlated to the measured dimension (Wenger et al., 2022). In order to quantify the fidelity, dimensions such as the fusion of filament, the diameter expansion of the extruded or the geometrical accuracy with respect to

the original g-code imported on the bioprinter are measured. Moreover, in-situ sensing can be useful to detect out-of-control states of the machine during the process.

In addition to this, monitoring in bioprinting involves additional factors other than the geometrical fidelity of the prints, which characterize this process with respect to traditional AM processes. These can be the in-situ monitoring of porosity or holes area with Magnetic Resonance Imaging (MRI) (Schmieg et al., 2022), the flow rate of constant pressure extrusion bioprinting with flow meters (Strauß et al., 2022), or eventually the monitoring of cell density deposition, achievable through fluorescence imaging.

Materials for cultured meat

Materials' constraints

The entire process of cellular cultivation above mentioned defines many constraints that must be respected by the materials used in the process. In particular, the constraints refer to the biomaterial used as substrate for three-dimensional cellular growth.

As discussed, TE for biomedical applications aims to produce functional tissues. Since they will eventually be implanted in the patient's, these tissues must not contain toxic metabolites, and must not be rejected by the organism. However, these constraints are particular only for biomedical applications, while for CM applications are negligible. The constraints of interest are those that can be commonly found in the biomedical and CM tissue engineering. In addition, some

more precautions have to be considered to extend the use of these materials to the food industry.

Firstly, most mammalian Stem Cells (SC) are anchorage dependent (Bodiou et al., 2020). The stronger they are anchored to their substrate, the more efficient will be their proliferation and differentiation. The attachment is regulated by the Cell Adhesion Molecules, that are represented by the Integrin family, the main surface receptor in SCs (Figure 16).

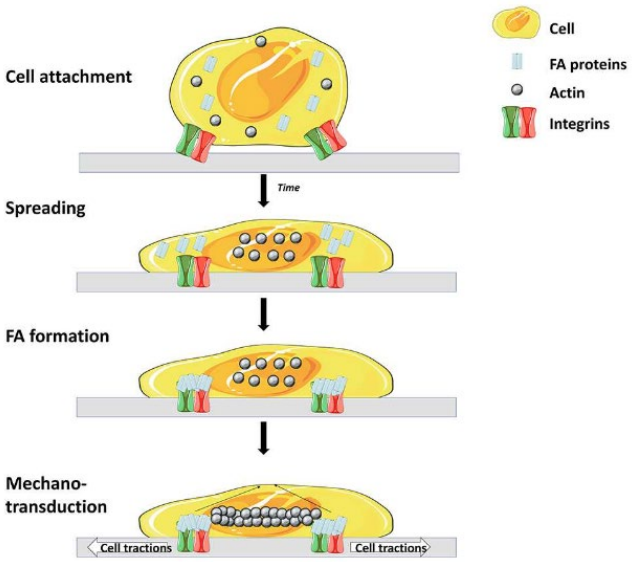

Figure 16: Cell differentiation process triggered by the cell adhesion on substrate (Source: Bodiou et al., 2020).

The material should therefore be a porous structure where cells can fit entirely, that provides the necessary functional groups for interaction with integrins and other Cell Adhesion Molecules to create anchorage sites along its structure. This translates in a common constraint for biomedical and food engineering applications often referred as biocompatibility: the compatibility of the biomaterial with the grafted organic tissue. In fact, the material - either if it used for scaffold production or in biofabrication - should mimic the Extra-Cellular Matrix (ECM) to enable cells to attach, proliferate and differentiate.

In order to be adapted to the biofabrication process, the material should satisfy the constraints of printability of the specific bioprinting technology adopted. Hence the material must have a rheological behavior that satisfies the extrusion and inkjet bioprinting, meaning that its viscosity has to belong to a certain range, or must be photocurable if it has to be processed through stereolithography or two-photon technique.

Focusing on the specific food industry constraints, in order to allow the material to be consumed as a food product, it has to be either removable, biodegradable, or edible. These three constraints refer to three different processing strategies for CM production.

In the first scenario, the material acts as a temporary substrate for the cellular activity, and at the end of the process it will be detached from the cells. To do so, the material should provide a high detachment yield, and has to be easily removable from cells. The detachment can be performed via enzymes, thermically, or mechanically without damaging the SC and the material.

In the second scenario, the material acts as a temporary substrate during the process, until — priorly to the end of the process — it gets degraded. This means that the material must perform degradation under specific condition, while remaining intact during the growing phase. The degradation can be started by chemical, physical, thermal, photo or biological initiation. This stimuli must be compatible with the SC, and not affect their viability.

Lastly, the material can be used as a permanent substrate embedded in the final product, that hence must be edible. In this scenario the material must comply with the strict food safety regulations, but can be also used to add sensory attributes, color, texture, or even taste to the final product (Bodiou et al., 2020). Hence in this case along with its edibility, the material should also perform good

textural properties, and guarantee thermal properties that are compatible with cooking practices.

In addition to this, a difference between the biomedical and food application of the material should be accounted for the volumes of production. In biomedical applications, materials are intended to produce tissues for specific use, often individually shaped: these may concern bone, cardiac or skin tissues made on demand for each particular case. On the other hand, in food application these materials would be used for scaled productions that are intended to meet – in the widest perspective - the world's population demand of meat. In this scenario the material's cost plays a tremendous role in its choice, making costly materials almost inaccessible for food purposes.

Table 1: Materials constraints for food and biomedical applications.

Biomedical Constraints	**Common Constraints**	**Food Constraints**
- Non-toxic for metabolism - Non-rejectable	- Biocompatible: porous structure with adhesion sites - 3D Printable	- Edible / Biodegradable / Removable - Inexpensive - Texture, color, taste, thermal properties (if edible)

Types of material for culture meat

Among the different class of materials, the one that by far achieved most efficiently the constraints for food bioprinting applications are the Hydrogels.

Hydrogels are three-dimensional (3D) polymeric networks that are filled with water (Lee & Kim, 2018). Their water content reaches 90-99% of the overall weight of the hydrogel and explains their high hydrophilicity and ability to safely

incorporate bio-logical entities (proteins and cells) without creating aggregates. The mechanical behavior of hydrogels is typically viscoelastic which is associated with the movement of polymer networks in the water (Lee & Kim, 2018).

They can be distinguished in physical (or reversible) hydrogels and chemical (or permanent) hydrogels. The former category refers to hydrogels where hydrogen bonds or hydrophobic forces play the main role in the molecular entanglement. This type of hydrogel can be dissolved with solvents easily. The latter refers to hydrogels where covalent bonds determine the molecular arrangement, thanks to the process of Cross-Linking. The strength of the covalent bonds of this type of hydrogels makes them permanently entangled (Figure 17) (Caló & Khutoryanskiy, 2015).

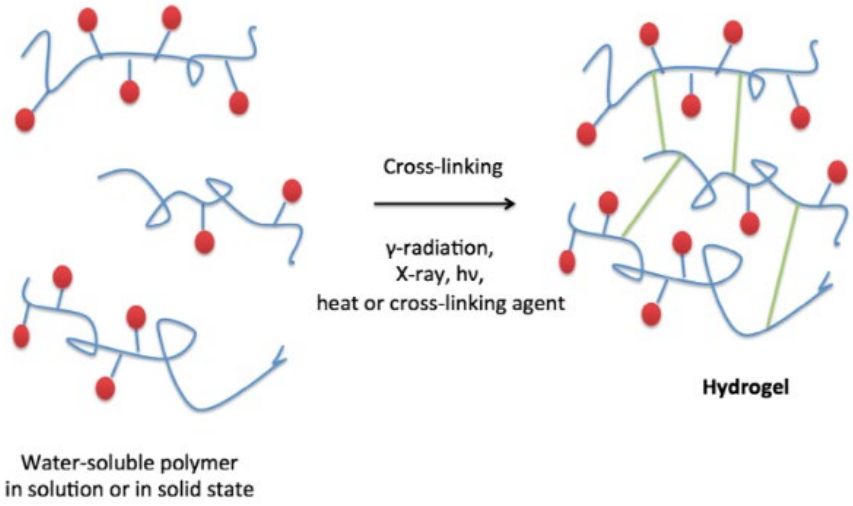

Figure 17: Cross-linking of polymer chains to form the Hydrogel (Source: Caló & Khutoryanskiy, 2015).

The formation of hydrogels starts dissolving in water original water-soluble polymers. The polymers are then crosslinked by a chemical, thermal, radiation or light stimuli. Once cross-linked the mechanical properties of the chemical hydrogel change, making them solid and resistant to permanent deformations;

physical hydrogels are otherwise easily relaxed when subjected to mechanical stressed.

The cross-linking ability of hydrogels opens the possibility to employ them in the bioprinting processes. For extrusion based and inkjet 3DBP, in fact, the hydrogel can be easily deposited in their non-cross-linked form, and once extruded can be cured either by UV light cross-linking or by a chemical cross-linking agent. For stereolithography, as well, a UV-curable water soluble polymers can be adopted and cross-linked locally thanks to the scanning laser.

The different type of water-soluble polymers used in the production of hydrogels can be classified primarily into plant-derived, animal-derived, and synthetic polymer, based on their origin. However, they can be further divided into four categories based on their structure: polysaccharides, polypeptides, lipids, and synthetics.

Polysaccharides

Among the most common polysaccharides we find starch, alginate, carrageenan, chitosan, cellulose, carboxymethylcellulose and pectin. Most of them have a plant origin, except for polysaccharides like chitosan that is extracted from prawn shells. In particular cellulose, chitosan and alginate are good candidates in the CM application due to their low costs and large availability.

These are polymers that do not contain natural anchor sites for the cell attachment. To enhance their biocompatibility with cells they are often modified with peptide-containing functional groups, which will incorporate the peptides like the sequence RGD, a macromolecule that interacts with the CAM on cell surface creating a “bridge” between polymeric chain and cell (Figure 18).

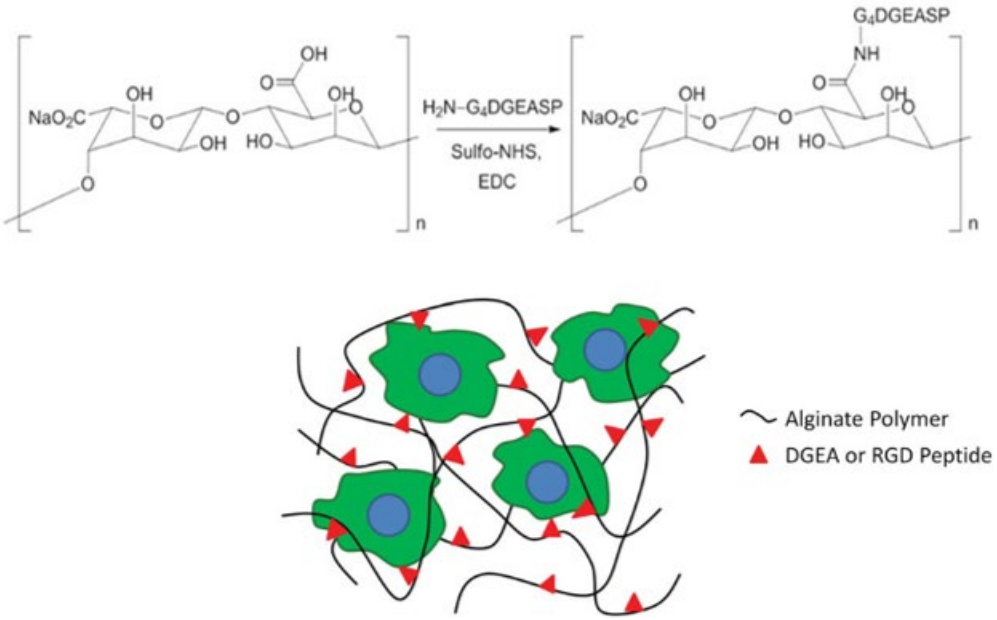

Figure 18: On top: example of Alginate chains modification with DGEA, an RDG motif alternative; on bottom: enhanced attachment in 3D cell culture (Source: modified from Mehta et al., 2015).

Polypeptides

The most adopted polypeptides are collagen, gelatin, and gluten. In this case collagen and gelatin find many applications in tissue engineering due to natural presence of the tripeptide motif RGD in their chains that make them suitable for cell attachment as is.

These polymers can be particularly interesting in the edible material application, when the hydrogel will be embedded in the final product. As they are quaternary polypeptide structures, they contain H-bond interactions that at elevated temperatures break, denaturizing the polymer structure. This can achieve interesting food applications as texturized components of the final product that melt during thermal processing (cooking).

Lipids

Among the lipids are manly used paraffin and shellac. As for peptides, they can be particularly interesting in edible hydrogels application. These polymers still find less applications in TE, but still can be found for their sensorial characteristics. Their application can achieve interesting textures and fatty flavors, which help resembling the characteristic fatty-flavor of conventional meat.

Synthetic / Composites

To the synthetic/composites family belong polymers such as poly lactic acid (PLA), poly lactic-co-glycolic acid (PLGA), poly ε-caprolactone (PCL), PGA and PEG. They are more appreciated for their mechanical properties with respect to the other polymeric families and are widely used as functional materials for biomedical applications.

However, for the food applications PLA, PLGA and PCL are often used as biodegradable hydrogels, while PGA, PEG, or even PLA can be used as an edible substrate, only when their synthesis is controlled in such way to not form undesired by-products (Bodiou et al., 2020; Seah et al., 2021). However, these polymers are non-bioactive and generally less biocompatible to natural polymers. Hybrid hydrogels can be preferred in order to overcome these issues.

State of the Art

In order to define an innovative and punctual Research Question, an extensive literature review was conducted among the different publications on the matter of CM. Since this topic is an innovation carried out simultaneously by public and private institutions, along with the research on scientific papers, books, and articles in the present study have been analyzed also the registered patents regarding the cultured meat sector.

The output of this literature review has been used to identify the literature strengths in the field of CM, and weaknesses. This way it was possible to identify a literature gap in which insert the research question of this thesis.

Research Methodology

A cascade approach was followed to identify the focus of the research. Therefore, starting from the widest range of publications and patents, the research was furtherly filtered up to reach only publications related to the specific topic of this work.

Concerning the Articles State of the Art (SoA) in the Literature Review, the main tool utilized was the online database of publications *Scopus.com*. Scopus is an abstract and citation database of peer-reviewed literature including scientific journals, books, and conference proceedings. This tool has been used to create logical queries in order to identify the publications related to that specific query. The logical queries were composed by keywords and the logic operators "AND", "OR" and "AND NOT". This way it was possible to create a complex research based on the interaction of the keywords.

For what concerns the patents SoA in the Patents Review, *Espacenet* was used as search engine. *Espacenet* offers free access to information about inventions and technical developments from 1782 to today. As for *Scopus.com*, *Espacenet* gives the possibility to browse patents through the advanced search tool, that uses logical queries allowing precise browsing among the different patents. As a supporting tool, the Good Food Institute provides a database containing all the companies involved in the cultured meat sector. This database was used as a reference for patent browsing, as contains information on the companies' location, founders, and core activity.

Literature Review

The first research carried out was the identification of the overall topic publications. The topic of CM was therefore researched with the combination of keywords "TITLE-ABS-KEY (cultured OR cultivated) AND TITLE-ABS-KEY (meat OR beef)". With this query, it was possible to identify all the articles present in the *Scopus.com* database that contained the words "cultured" or "cultivated" in their titles, abstracts, and list of keywords, together with the words "meat" or "beef". It was chosen to search both for "cultured" and "cultivated" since these are both terms used in the identification of the topic of cellular cultivation, as for "meat" and "beef" that both can be found in literature regarding this topic.

This prior research results in 2796 articles that matched the conditions. Interesting about this first research is the trend in publication over the years. This research demonstrates the novelty in the topic, since the pick of the curve is represented by the year 2021, due to the fact that this literature review has been carried out in 2022, and therefore the number of articles of this year is still increasing (Figure 19).

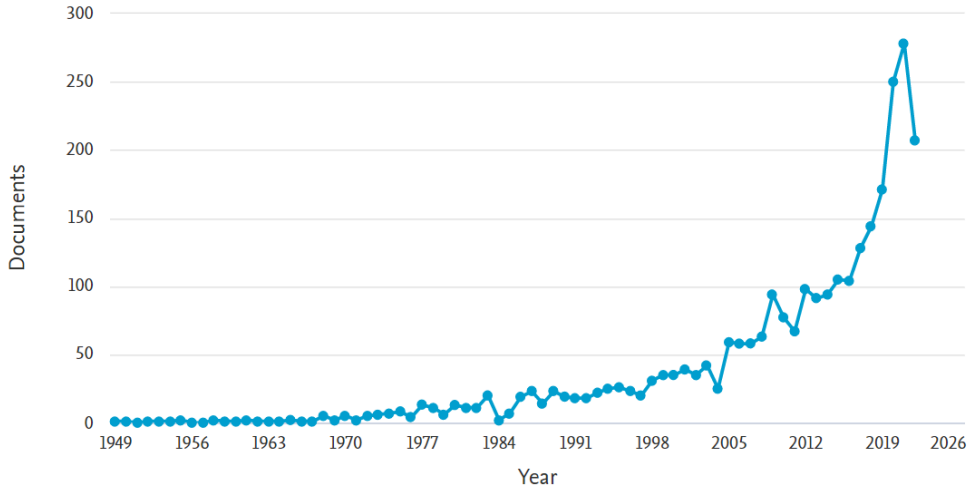

Figure 19: Documents by year in the preliminary research (Source: Scopus.com).

It is possible to identify that the exponential growth of the curve started around year 2012, probably due to the mediatic resonance of the public presentation of the first cultivated hamburger in 2013 by Mark J. Post, founder of Mosa Meat (O'Riordan et al., 2017).

In fact, another interesting result in the preliminary research is the number of publications by author. Again Mark J. Post is the author with the highest publications related to the topic of CM (Appendix 5). This result also demonstrates the commitment of private institutions in the research of CM, since Mark J. Post works in the company Mosa Meat.

The subject areas of this topic are very variegated. Among them, however, "Agricultural and Biological Sciences" is the subject area with most publications related to. In fact, within the preliminary research have gotten many articles related to agriculture that matched the first two terms "cultured" or "cultivated", but that had also "meat" or "beef" as secondary words in the abstract matching the query of this research (Figure 20).

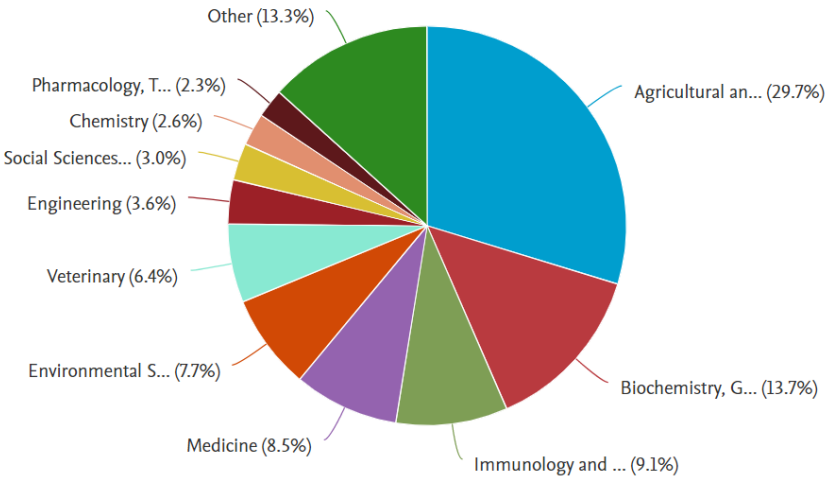

Figure 20: Publications by subject-area (Source: Scopus.com).

Nevertheless, among the "Agricultural and Biological Sciences" category are also listed publications that explore the biological issues related to TE. Together with this category, the biological issues are also listed in the publications belonging to "Biochemistry, Genetics and Molecular Biology" that is the second most discovered subject area, and "Immunology and Microbiology", as third. Additionally, related to the biological and microbiological issue are also listed the subject-areas of "Medicine", "Veterinary" and "Pharmacology, Toxicology and Pharmaceutics". This means that cumulating all these subject areas, 69.7% of publications are focused on issues that explore the topic from the biological point of view, with issues as the substitution of Fetal Bovine Serum (FBS), generation of cellular lines optimized for the cultivation on scaffolds and hydrogels, or genetic modifications of cells that enhance their proliferation and differentiation efficiency.

Interestingly, only 3.6% of the publications belong to the "Engineering" area, whereas 62.5% of them are related to "Chemical Engineering". In fact, most of the engineering interest in the CM sector is dedicated to the scaling-up of the bioreactor stages, which are common issues in the chemical engineering industry.

However, less interest is dedicated to the scalability of the other processes, such as biofabrication and more generically three-dimensional tissue generation.

To explore the portion of the literature dedicated to 3DBP, a second iteration was done. The query has been adjusted to "TITLE-ABS-KEY (cultured OR cultivated) AND TITLE-ABS-KEY (meat OR beef) AND TITLE-ABS-KEY (printing OR bioprinting)". The keyword "3D" was not inserted in this research as would incorporate misleading papers and exclude publication referring to it as "three-dimensional" or other many synonymous. This iteration of the research has submitted a total of 26 publications related to 3DBP.

Another iteration at this level was done, in order to verify how much of the engineering-related literature refers to scaffolding technology instead. Changing the query to "TITLE-ABS-KEY (cultured OR cultivated) AND TITLE-ABS-KEY (meat OR beef) AND TITLE-ABS-KEY (scaffolding OR scaffold)" gives 46 resulting articles, demonstrating the higher interest in this technology, rather than bioprinting.

Moreover, in order to identify if other publications were cut out by the second iteration, a third iteration was conducted with the query "TITLE-ABS-KEY (meat OR beef) AND TITLE-ABS-KEY (printing OR bioprinting)", that omitted the words "cultured" and "cultivated" in order to identify possible publications using analogous keywords. This resulted in 228 publications, but mainly out of the cellular agriculture topic as predictable (despite the 26 publications of the previous iteration that were included in this one as well). This iteration, indeed, included literature regarding the meat analogues, but with plant-based ingredients. This sector is another novel and appealing application of AM in the protein alternative sector, where vegetable proteins are extracted in powders, and compounded with liquid additive to form inks that are subsequentially 3D

printed. Many companies are investing in this technology like the Israeli Redefine Meat or the Spanish Nova Meat. Due to scalability of the process, and to the absence of regulatory barriers this technology gained much more popularity than CM. Moreover, as for AM applied in CM, this technology unlocks the possibility of creating multi-material products, which resemble in a more realistic way the real meat muscle structure rather than other plant-based alternatives.

Focusing now the 26 publications of the second iteration about AM application on CM, further considerations can be done. Firstly, analyzing the document type it is possible to understand the type of publications (Figure 21).

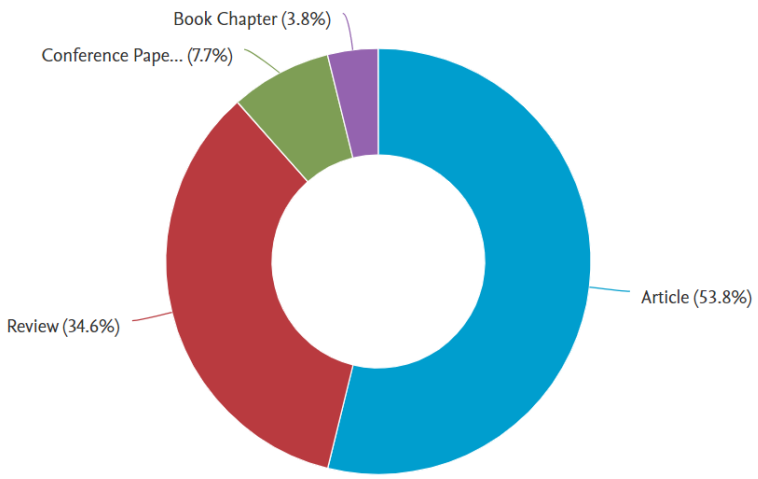

Figure 21: Publications by document type (Source: Scopus.com).

In fact, 9 of these publications are reviews on the CM topic, that do not explore specific technologies or techniques, but rather collect the already existing knowledge on the sector, explaining the potentiality of this topic and what the literature is currently focused on.

In particular, the most relevant of them are reviewed below as they elucidate key concepts that help in understanding the potentiality of the process.

The review proposed by Levi et al. analyzed electrospinning, texturized proteins, plant tissue decellularization, edible microcarriers, cell sheet engineering, and 3D printing as technologies that are mostly appreciated for the development of scaffolds for CM. In particular, 3D printing gets critically reviewed in all the different processes, such as extrusion-based, inkjet, LAB, and STL. Only extrusion-based 3D printing is considered as a potential competitor of electrospinning in the generation of scaffolds for CM. Together with the analysis of the process, the review explores the different biomaterials that can be used in the process and their advantage.

In the work of Lanzoni et al., all the challenges related to the process of culturing meat through 3D bioprinting or scaffolding are collected. The review gathers both the biological and the engineering challenges of the process, whereas about the latter are discussed all the advantages and disadvantages of the different 3D bioprinting techniques. The review also gives a detailed description of the process parameters during 3D bioprinting, and how they affect the final viability and cell density of the product. Additionally, all the possible biomaterial categories are descripted, with real examples of bioinks that can be adopted in the 3D bioprinting process.

Yang et al. described the potentiality of chitosan and whey protein bioinks in a systematic review. In this work the process of 3D printing is briefly described, to later investigate in depth the function of chitosan in the food industry, its appreciable properties, and its drawbacks in terms of printability. Whey proteins are proposed as a food additive that could improve the printability of this material and enhance the nutritional properties of the final product.

The review of Bomkamp et al. focused on biomaterials for the production of scaffolds. The review firstly discloses the structure of muscles in mammals and

fish, and later explains the role of its components as the muscle fibers, intramuscular fat, and the importance of ECM (Extra Cellular Matrix). The review then describes the different methods to process cultured meat, and how the properties of the biomaterial can be exploited to achieve the best results in each of them. 3D printing and bioprinting are analyzed briefly without a particular focus, describing the usefulness of hydrogels for such technology.

K. Handral et al. breaks down the process of culturing meat with 3D bioprinting in all the sub-processes, providing a well detailed guide of the process, and its applications, like the pioneering application of cultured meat in space missions. Along with that, the review also analyzes the process parameters that affect the printing process and the related challenges for 3D bioprinting in food applications.

Jo et al. take into analysis the technologies to assemble a 3D tissue, which are electrospinning, cell layering and 3D bioprinting. In this review, these technologies are described, together with their advantages and disadvantages. Regarding 3D bioprinting, other than extrusion, inkjet and stereolithography is propose the spheroid assembly, a process where pre-cultivated spheroids are used as building block of three-dimensional deposited tissues. All the different technologies are compared critically, in order to underline their advantages with respect to the others.

Although being complete works that cover most of the aspects involved in the CM 3D bioprinting process, these reviews do not contribute with innovative solutions, but rather collect the pre-existing knowledge about this sector. On the other hand, interesting articles are provided in this iteration of the literature review, with innovative solutions in this process.

In the article of Lindner & Blaeser are presented the potentiality of scalability in 3D bioprinting with the help automated process. It discusses the hardware, sensors, and automation potential of bioprinting in the different scenarios of application, like the food industry. However, this work is limited to the description of the equipment involved in the automation and doesn't provide any practical example of bioprinting of cultured meat.

A really interesting work is provided by Dutta et al. where an Alginate-Gelatin-Protein Hydrolysate hydrogel is explored as a suitable bioink for 3D Bioprinting of CM. Both pant proteins and insect proteins are tested as possible additives in the Alginate-Gelatin bioink and are processed through extrusion-based bioprinting. The printing happens in a pre-gelatinization Pluronic bath where the extruded ink could keep its shape without collapsing, and afterwards, the constructs were properly cross-linked via a chemical cross-linking agent. It was demonstrated that the novel ink not only provided the desired printing stability (due to the addition of Protein Hydrolysate), but also enhanced the overall viability of the cells after print.

In the article of Ianovici et al. is described the use of RGD-modified Alginate with Pea and Soy proteins hydrogels, for the production of scaffolds either by 3D printing or mold-based. However, due to the scaffolding approach, none of these two approaches comprises a cell-laden hydrogel deposition, making the step of seeding still necessary along the process.

In their work, Li et al. aim at producing a cultured pork meat with the use 3D Bioprinting. They propose the use of Alginate-Gelatin and Gelatin Methacrylate-Silk Fibroin for the production of hydrogels to be used in extrusion-based 3DBP. The first bioink was cross-linked by chemical cross-linking agent ($CaCl_2$), while the second, due to the Methacrylate modification of Gelatin, was cross-linked via

UV light. The second bioink demonstrated higher differentiation level, due to the presence of silk fibroin that created an environment favorable for cell elongation.

Kang et al. propose in their work an innovative extrusion based bioprinting approach, where the material is deposited immersed in a gelatin matrix, along the z-axis. The gelatin matrix acts as a structural support for the vertical deposition, and also integrates a tendon-like portion at the end of the fibers that enhance the fiber tension, triggering the differentiation via mechanical stimuli. This bioprinting approach, called tendon-gel integrated bioprinting (TIP), achieves an outstanding differentiation level of the bovine stem cells, creating well-aligned fibers along the printing axis. This work is in fact cited in almost all the reviews that explore the potentiality of 3D Bioprinting for CM due to the incredible resemblance to the real meat of their result, and the process efficiency achieved. However, it has to be noted that this process presents many difficulties, due to the printing along the z-axis, making it hardly scalable when compared to conventional x-y-axis deposition.

Table 2: Iterations' results of the articles and review state of the art.

Iteration	Query	Results
1ST	TITLE-ABS-KEY (**cultured** OR **cultivated**) AND TITLE-ABS-KEY (**meat** OR **beef**)	2796
2ND SCAFFOLDING	TITLE-ABS-KEY (**cultured** OR **cultivated**) AND TITLE-ABS-KEY (**meat** OR **beef**) AND TITLE-ABS-KEY (**scaffolding** OR **scaffold**)	46
2ND 3D BIOPRINTING	TITLE-ABS-KEY (**cultured** OR **cultivated**) AND TITLE-ABS-KEY (**meat** OR **beef**) AND TITLE-ABS-KEY (**printing** OR **bioprinting**)	26
3RD	TITLE-ABS-KEY (**meat** OR **beef**) AND TITLE-ABS-KEY (**printing** OR **bioprinting**)	228

Patents Review

The patents SoA analysis started with the Good Food Institute's alternative protein database. The Good Food Institute (GFI) is an international nonprofit reimagining meat production, aiming to spread knowledge for investors and companies in order to make alternative proteins the substitute of livestock meat. The GFI provides an open platform database, containing information on more than 1000 companies involved in the protein alternative sector worldwide, continuously updated.

Starting with the 1090 companies involved in protein alternative, it was possible to identify the 89 companies that correspond to the filter "Protein Category: Cultivated". It was then created a sub-database, containing the information regarding these 89 CM companies, as a starting point to later browse all the related patents on Espacenet. For each company was collected the information regarding the company name, brief description, protein category, company focus, technology focus, product type, animal-type analog, ingredient type, operating regions, country/province, state, city, website, year founded, founders. On Espacenet, using the Advanced search tool, were collected all the patents resulted by searching either the name of the company, or the names of the founders, in the research field "Investors or Applicant".

A total of 47 patents were collected and analyzed individually (Appendix 1).

Each of one was collected along with its corresponding company, technology used by the company, and brief description of the innovation.

Among all the patents, only Meatech 3D described explicitly their 3D Bioprinting approach and technology. In their patent, Fima et al. claim a computerized 3D Bioprinting system, with a conveyor belt able to operate in continuous,

introducing an innovative breakthrough to the conventional "batch" approach, typical of the AM. The bioprinter is inkjet, with multiple nozzles able to print multiple materials at the time. The patent claims that the printer has at least three nozzles: the first is connected to a cell-laden bioink reservoir, the second to a functional bioink reservoir, and the third is a cross-linking agent for chemical curing. The patent provides also eight bioink formulations that are used in this process, either for being embedded with cells, or to be the functional support. Among them, alginate and gelatin are the most used materials in these bioinks.

The printing process involves the deposition of the first layer of the second bioink, which is the structural material, and the curing of it by the third printhead containing the cross-linking agent. Subsequently, the first bioink is deposited on the surface of the structural layer and is cured. Following this structure for all the layers will eventually generate a product with alternated layers of structural material and cell-laden material.

Conclusions and Literature Gaps

Cultured meat is clearly an appealing topic of the latest years, with an increasing trend of publications, and interest by investors. As seen during the different article's literature review iterations, most of the effort right now is devolved in biological issues rather than the engineering ones. It reflects that the focus of the research is still at laboratory scales, rather than the industrial scaled up scenario. This is a result of the low scales of the actual productions since —due to the high costs and few regulations — in very few cases cultured products are sold in the market.

Focusing on the literature and patents available on CM's engineering implication, further considerations can be done. Firstly, scaffolding technology is

by now favored on 3DBP. In fact, both the scientific papers and the patents are in the majority focused on technologies to produce scaffolds rather than AM biofabrication techniques which are still considered a novel approach for this process.

Even if companies such as Meatech 3D already invest on this technology, 3DBP is still facing issues and limitations that scaffolding on the opposite has already overcome. In fact the maturity of the technology makes it more appealing for a laboratory scale production, but looking at the scalability it still can't overcome the big limitation of the small diffusion depth of cells (Lanzoni et al., 2022).

Despite the progress made for biomedical applications, research relating to Bioprinting for CM purposes is still in an infancy stage, as requires non-animal derived, printable and potentially edible materials (Ianovici et al., 2022). In fact, most of the articles proposed in the SoA simply discuss about the potentiality of the 3DBP technology without introducing new materials (Jo et al., 2021; K. Handral et al., 2022; Levi et al., 2022), or otherwise describe new technologies but without focusing on the material (Kang et al., 2021).

Few works are still very relevant but present their own criticalities. In the patent provided by Meatech 3D are proposed many bioink formulations, however these refer only to inkjet bioprinting, that works with low viscosity materials, making them unsuitable for extrusion based applications, which are the most common (Fima et al., 2020).

In their review, Yang et al. claim that there is a lack of a systemic review about bio-inks for 3D/4D printing applications. In their work they analyze the potentiality of a Chitosan-Whey Protein bioink for the food industry, however the structure of the work is still a review, so, as mentioned before, it does not add any practical information on the use of such material to the literature.

Moreover, none of the works of the SoA explore the printability of the proposed materials, limiting the process optimization. The printability assessment of bioinks is a fundamental approach to identify the right configuration for the achievement of quality. The printability assessment is usually considered the starting point in the definition of a material from an AM point of view (Hölzl et al., 2016; Paxton et al., 2017) in fact, in order to achieve the best processability, the material has to be fully defined in its printing behavior.

Without this level of control on the material behavior, however, the process of bioprinting may become very complex and difficult. This affects both its operability — making it inefficient, slow, and non-continuous due to interruptions like clogging — and in final results quality — like the presence of errors that make the product unsuitable, or bad configuration of the construct that limits cellular growth. This can lead to a miss confidence for the 3DBP process, as for the work of Levi et al. where bioprinting is considered unreliable and problematic due to its continuous occurrence of problems. However, none of the works reported in the SoA put their basis in the printability assessment.

Research Question

This thesis aims at presenting the first empirical printability model that identifies the optimal window of printing parameters considering the model's uncertainty, in order to guide the experimenter according to any objective functions.

In particular, this works aims at assessing the printability of edible biomaterials suitable for 3DBP for CM purposes. The printability results will be elaborated with a statistical data analytics approach to produce a regression model and a probability map to make reliable predictions on the final quality of the prints. This statistical approach was pursued since there is a lack of literature regarding printability assessment for edible bioinks, and in particular no work integrates an analysis of the prediction uncertainty likewise this thesis with the formulation of the probability maps.

The bioprinting technique chosen for this work is the extrusion-based due to its ease and high presence in the TE scenario. Among the different bioprinting technologies it has the highest versatility and does not need a photo-curable material. The last aspect in particular helps in the development the edible material, since no photo-initiators are needed, which are compounds that do not have a certified edibility verification.

Regarding the material, Alginate was chosen as basis for the biomaterial of this research. Alginate is a polysaccharide, that is a chemically cross-linkable material, a fundamental aspect for the extrusion based bioprinting. Alginate was chosen since is a common material found in the food industry, and therefore its edibility is already well established. It is cheap with very high availability making it the best candidate in the scalability optic of CM. In addition, alginate

is already widely used in the biomedical 3DBP, and it's already been appreciated for its printing behavior.

However, Alginate's main drawback is its low biocompatibility with cell. This material does not have anchor sites that promote cellular growth and differentiation. Usually, in the biomedical literature, the problem is overcome by the chemical addition of RGD peptides sequence on the polymer backbone, however this modification is achievable only by carbodiimide chemical reactions (Bidarra et al., 2011), that still does not have the certification for food use (Bodiou et al., 2020) and increase importantly the cost of the material.

This is why it was chosen to explore also composite materials, with alginate as main component. The choice fell on Alginate with Gelatin. As mentioned in the chapter "Types of material", Gelatin is appreciated for its natural presence of RGD-containing amino acids, that provide the best interaction between the cell's integrin and the biomaterial net. Thus, the integration of Gelatin in an Alginate hydrogel will enhance the biocompatibility of the material, keeping its capability of cross-linking chemically. Additionally, as for Alginate, Gelatin is a widespread material with low costs, keeping valid the possibility to scale up the production of CM containing it.

Therefore, according to the chapter "*Materials' constraints*", the choice of using pure alginate and alginate compounded with gelatin satisfies all the desired constraints of edibility, printability, biocompatibility, and economic feasibility.

Materials and methods

In the following section are collected all the materials and the methodologies adopted for the elaboration of the results. In particular, the section "*Materials*" contains all the information about the bioink solutions and equipment of the bioprinter, the section "*Design of experiment*" describes the analytical approach adopted to obtain statistically significant results, and the section "*Data collection*" describes the process of data gathering from the raw images collected.

Materials

Stock Solutions

To produce the two bioink formulations, two stock solutions were prepared.

The alginate 8% (w/v) stock solution was prepared dissolving Sodium Alginate (purchased from Sigma Aldrich) in sterile PBS. The solution was then continuously stirred at 50°C for 4 hours with a heated magnetic stirrer, to achieve the complete hydration of the sodium alginate powder.

The gelatin 16% (w/v) stock solution was prepared dissolving Gelatin type A (purchased from Sigma Aldrich) in sterile PBS. The solution was then stirred at 30°C, with particular attention in not trespassing this temperature otherwise the gelatin would denature. The stirring was achieved with a heated magnetic stirrer, for 4 hours to completely hydrate the powder.

Alg bioink

The first bioink for the experimentation is alginate 6%, referred as Alg. To produce it, the alginate 8% stock solution was diluted with sterile PBS in a ratio

3/1 to form 40 ml of solution. To the mixture were also added 2 ml of Amaranth 10% (w/v) in order to turn the colour of the solution into a vivid red. The mixture was then stirred with a magnetic stirrer until homogeneous.

Alg+Gel bioink

As second bioink was used a compound of alginate 6% and gelatin 4%, referred as Alg+Gel. This bioink was produced mixing the stock solution of alginate 8% with the stock solution of gelatin 16% in a ratio 3/1 to form 40 ml of solution. To the mixture was added 2 ml of Amaranth 10% (w/v) to turn the colour of the solution into a vivid red. The mixture was subsequently stirred until homogeneous with the help of a magnetic stirrer.

Bioprinter

The bioprinter used for this thesis was the BIO X ™ provided by Cellink. This bioprinter has a printhead able to scan along the x-y plane and a print bed moving along the z axis. The printhead features three tool slots in which can be inserted either a pneumatic extruder without temperature control, a pneumatic extruder with temperature control, an inkjet extruder, a piston extruder, a fused filament extruder and a HD camera. This bioprinter is capable of controlling the temperature of the nozzle and print bed.

For this experiment the bioprinter was equipped with the pneumatic extruder with temperature control together with the HD camera. The nozzle used for this experimentation was a conical nozzle with 0,410 mm diameter of extrusion. The third slot was kept empty since no other tool was required. The bioprinter was held in a laminar fume hood with sterile environment. All the accessories required for the bioprinting (cartridge, nozzles, bioprinter components) were acquired from Cellink.

3D modelling

The 3D model imported on the BIO X was designed on Autodesk Fusion 360. Once designed, the model was exported as a stereolithography file (.stl), and directly imported on the bioprinter with a USB stick.

The slicing of the 3D object was performed by the BioX bioprinter, which has a CAM software integrated in the software. The different parameter of the slicing were inserted through the touch screen interface. In particular the infill density was set at 25%, with squared pattern, and the first layer height at 80% of the nozzle diameter.

Image analysis

The image analysis algorithm was developed on MATLAB R2022a (Appendix 6). The images were gathered by the bioprinter HD camera tool, imported from the BioX to a PC with a USB stick and imported on MATLAB R2022a.

The organization and enumeration of pictures was also performed by an algorithm developed on MATLAB R2022a.

Data analysis

The data gathered from the image analysis software were imported and analysed on Minitab Statistical Software. The analysis was also supported by Excel spreadsheet.

The data representation was done both with MATLAB R2022a and Minitab, depending on the type of graphs: the former for all the 3D surface plots and colormaps, and the latter for the individual values plot, normality test plot and autocorrelation function plots.

Design of Experiment

In order to explore the printability of the proposed bioinks, a two-factors factorial design of experiment was adopted.

In a two-factors factorial design there are *a* levels of factor *A* and *b* levels of factor *B*, which are arranged in a factorial design: each of the *n* replicate of the experiment contains all *ab* treatment combinations (Montgomery, 2013). For the development of this experiment the two factor chosen were the pressure of extrusion of the pneumatic extruder (P), and the velocity of scanning of the print head (v) (Figure 22). It was chosen to explore 6 levels for both the factors, for 3 replications, with randomized data collection. This resulted in 108 prints for each of the 2 bioinks.

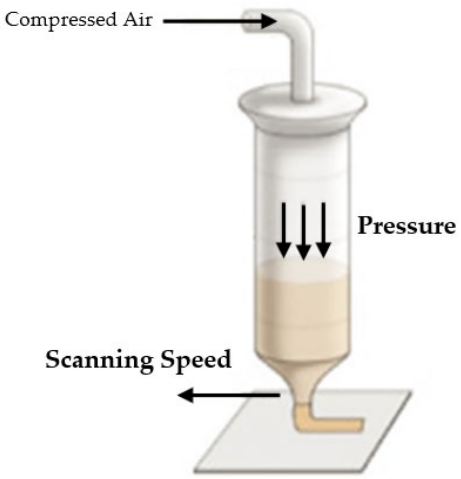

Figure 22: Schematics of a syringe-like cartridge and the influence of pressure and scanning speed (Source: modified from Agunbiade et al., 2022).

The pressure, expressed in kPa, defines the overall force applied on the syringe-like cartridge back by the compressed air, divided by the cross section area of the syringe. The higher is the pressure, and the higher will be the expected flow rate of bioink extruded through the nozzle. In the other hand, the lower the pressure,

the lower will be the expected flow rate, with a low limit value of pressure below which the shear stress induced by the nozzle inner walls will overcome the pressure of the compressed air, and no extrusion will be achieved.

The 6 levels of pressure taken under consideration were 5, 10, 15, 20, 25 and 30 [kPa]. The interval spaces between 0, which is the critical case in which no pressure is applied to the bioink, with a resulting absence of extrusion, and 35, a value of pressure over which it was experienced from previous experiments that the amount of ink extruded is excessive incurring in the problem of over extrusion, together with the risk of fatally damaging the cells, since they are sensible to shear stresses (Boularaoui et al., 2020).

The scanning speed of the printhead, expressed in mm/s, defines the speed of travel of the print head along the deposition direction. From this value is dependent the extruded filament thickness due to the independency between the scanning speed and the extrusion flow rate: at high scanning speed the extruded filament will be thinner (due to the spreading of the same amount of material in a longer distance), while at low scanning speed the extruded filament will be thicker (due to the spreading of the same amount of material in a shorter distance). For the case of the scanning speed there is an upper limit. It is defined by the velocity over which the print head will be no longer accurate due to the excessive shaking of the machine (caused by the inertia of the rapid changes in direction at high speed of the print head), making the final construct unsatisfactory.

The 6 levels of scanning speed taken under consideration were 5, 10, 15, 20, 25 and 30 [mm/s]. The interval spaces between 0, which is the critical case in which the print head would be stationary, and therefore no construct would be formed, and 35, a value over which the printer will be subjected to excessive oscillations.

The data collection sequence was randomized along both the levels and the replications. To do so it was used the Minitab tool "Design of Experiment", that creates the randomized sequence of interactions Pressure/Scanning Speed suitable for statistical analysis. The randomization avoids the effects of autocorrelation, that would happen if the data were collected sequentially.

The temperature of the nozzle was kept constant at 22°C (simulating ambient temperature) during all the experimentation. This temperature was chosen in order to minimize the temperature control effort, with a consequent energy saving. In fact, with a nozzle operating at a temperature similar to the environment temperature, the heater of the closed-loop controller will consume low amounts of energy; the same applies to the cooling fan. For the aim of this experiment, the print bed temperature was not controlled at all, as it does not affect the process but either the cell viability.

Data collection

The data collected during the experimentation was the Printability Index (PI). This index represents the fidelity with which the printer is able to represent the input geometry provided by the g-code, which is the file containing all the instructions that the printer has to follow in order to produce the desired 3D model. The PI can be evaluated as the ratio of the real area of the void, over the area of the ideal void imposed by the g-code (Ouyang et al., 2016).

$$PI = \frac{A_{real}}{A_{ideal}} \quad (1)$$

The domain is $PI \in [0, +\infty]$, and is divided in 3 situations: $PI < 1$, the case in which the real area of the void is smaller than the ideal area; $PI = 1$, the case in

which the real area of the printed void is equal to the ideal area; $PI > 1$, when the area of the void is higher of the ideal area (Figure 23).

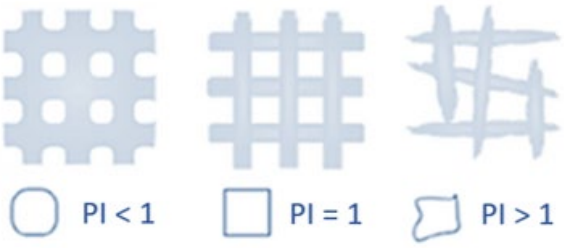

Figure 23: The 3 cases for PI (Source: modified from Compmech Università di Pavia).

In the first case fall all the situations in which occurs the over extrusion. This means that the amount of bioink extruded is higher than the correct amount needed to print the geometry. At worst, the value of PI is equal to 0, meaning that the over-extrusion was enough to completely fill the void, resulting in $A_{real} = 0$.

In the third case are included the cases of under extrusion. This is the situation in which the amount of bioink extruded is not enough to correctly print the geometry. In this domain also fall the cases in which the under-extrusion causes the discontinuity of extrusion, generating voids along the printed filament. At worst the printer does not extrude any material, meaning that the A_{real} is unquantifiable, and tent to $+\infty$.

The second case eventually represents the optimal situation where the amount of bioink extruded is equal to the amount needed to correctly print the geometry: in this situation neither over nor under extrusion occur. However, due to the nature of the variable, is very unrealistic that PI reaches the exact value of $PI = 1$ (this can happen only if $A_{real} = A_{ideal}$). This is why it can be actually identified an interval around 1 in which the value of PI is assumed to be optimal. For this experimentation, the optimal interval was chosen as $PI \in [0{,}75; 1{,}25]$.

As mentioned, the ideal area is a design parameter that was predefined and fixed for all the experimentation, since it was used the same g-code for all the printed objects. The real area of the printed void, instead, needed to be measured. To do so an image analysis approach was pursued.

First of all, a suitable geometry for this experiment was designed. The object was designed to be one layer thick with a rectangular geometry, that when processed by the CAM software would have been transformed into a net-like geometry with squared voids. Using the HD camera tool of the bioprinter, at the end of each print it was possible to capture a picture of the printed object (Figure 24).

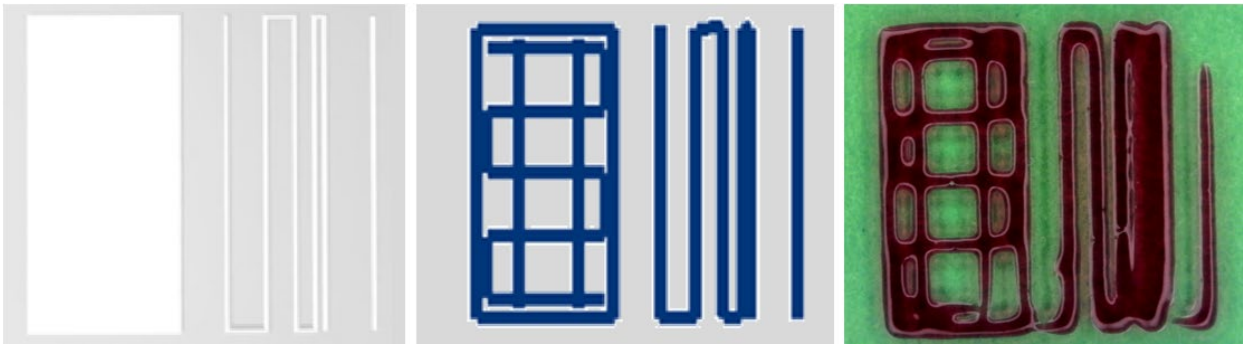

Figure 24: On the left the input geometry to the bioprinter created with Autodesk, on the center the g-code pattern generated by the CAM software with 25% of infill density, on the right the picture of the printed object taken with the HD camera tool.

The collected images were then analyzed with an algorithm developed on MATLAB R2022a. In order to identify the real area of the voids, the algorithm separated the red filament from the green background though an image segmentation approach.

The segmentation was done both using an RGB channels separation approach, and a region growing approach (Appendix 6). The output of the two segmentation approaches was then merged and used to create a mask for all the voids, which was used to calculate its area in pixels. The PI was then calculated

as the number of pixel of the measured area, divided by the number of pixel of the ideal area given by the g-code (Figure 25).

Once calculated the value of PI for all the 4 voids of the 3D model, the overall value of PI of each print was determined as the mean of the 4 values of PI of the single voids and named as Average Printability Index (API).

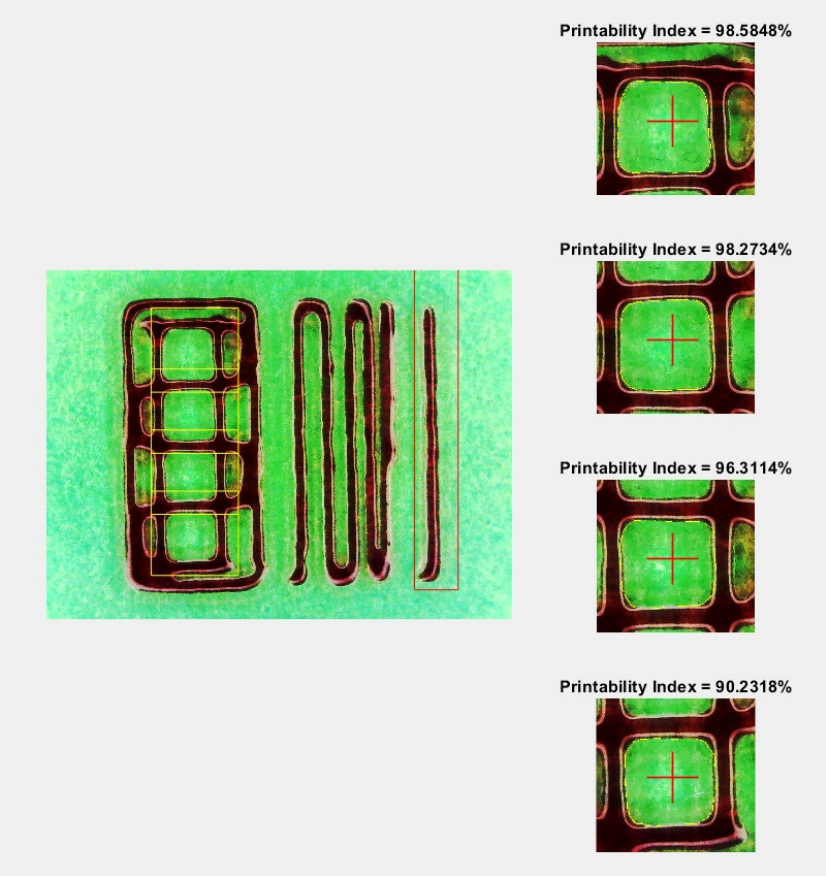

Figure 25: Evaluation of the PI of a print, using both the RGB channel separation and region growing approach. On the left the initial image with the yellow squares indicating the cropping regions, on the right the four cropped regions with the red cross indicating the seeding point of the region growing approach, and in thin yellow line the contour of the area of the void identified by the algorithm.

In practice the values of the API do not rage in the entire domain of PI – which is $PI \in [0, +\infty]$ - but ranges between two saturation values that are a minimum of

0 and a maximum of 303. The lower limit 0 as already discussed represents the case in which the void of the printed object is completely filled by the bioink. The upper limit 3.03, instead, represents the opposite case in which no ink got extruded. However, in this situation the value of API does not reach $+\infty$ due to the image analysis approach: indeed, the area in which the void is inspected (the cropped regions in Figure 25) is 3.03 times larger than the ideal area of the void. This means that when there is no extrusion, the algorithm recognizes all the background of the cropped region as void area, which can be at maximum 3.03 times the ideal area of the void (Figure 27).

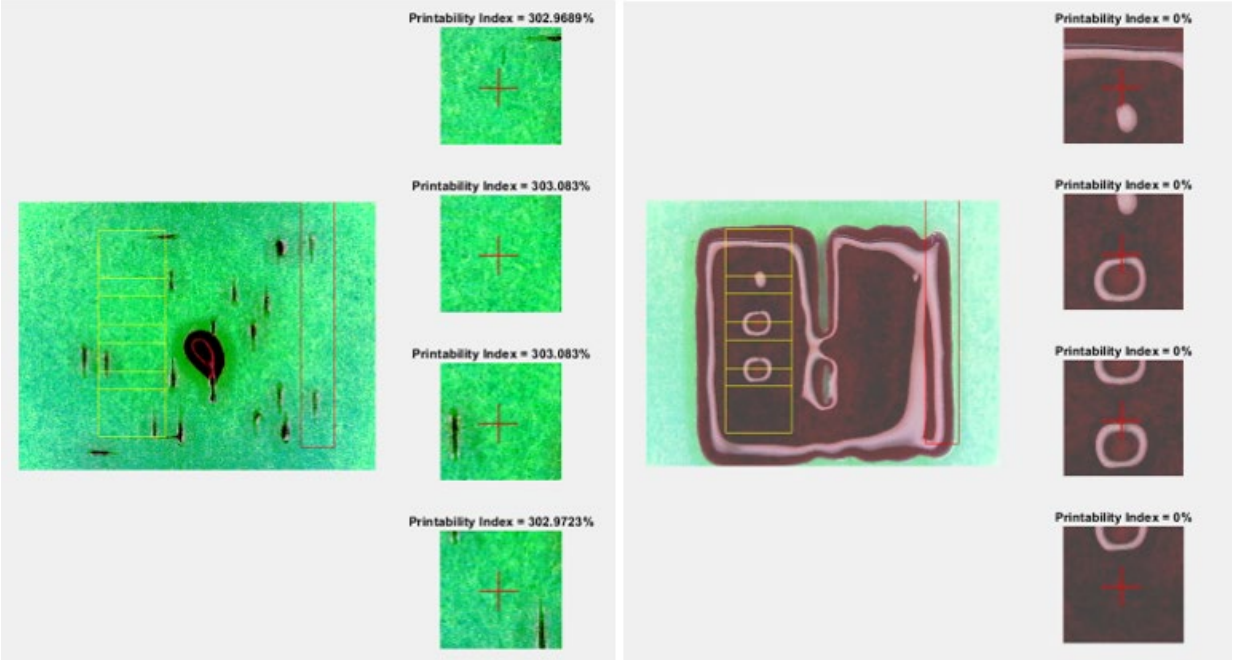

Figure 26: On the left the saturation case of no extrusion resulting in a value of PI=3.03, on the right the saturation case of over extrusion, in which the voids are completely filled by the bioink resulting in a value of PI=0.

Results and discussions

Once measured all the values of API, the datasets were imported on Excel, reorganized and subsequentially imported on Minitab for the data analysis.

This section aims at describing the process followed to identify the most suitable models that describe the relationship between the API and the pressure and scanning speed on the process.

During the collection of the images, it was observed that the behavior of the three bioinks with respects of the pressure and scanning speed was similar, but with a bias between each other. Since in fact the two cases of the experiment represent the same phenomena, but observed using two different bioinks, it was forecasted prior to the development of the models that they would have had the same regressors but with different proportional constants. This forecast was then confirmed by the practice, as the output models followed the same dependences with high significance.

This is why in the analysis of the Alg+Gel model is described the process of identification of the regressors in depth, while in the following case of Alg are used the same regressors achieving a similar model.

Hypothesis of the model

For both the models was adopted the linear regression modelling methodology. The parameters were estimated with the least squares method using the software Minitab.

The model equation may be written in matrix notation as following (Montgomery, 2019):

$$\boldsymbol{y} = \boldsymbol{X}\boldsymbol{\beta} + \boldsymbol{\varepsilon} \tag{2}$$

Where:

$$\boldsymbol{y} = \begin{bmatrix} y_1 \\ y_2 \\ \vdots \\ y_n \end{bmatrix}, \quad \boldsymbol{X} = \begin{bmatrix} 1 & x_{11} & x_{12} & \cdots & x_{1k} \\ 1 & x_{21} & x_{22} & \cdots & x_{2k} \\ \vdots & \vdots & \vdots & \ddots & \vdots \\ 1 & x_{n1} & x_{n2} & \cdots & x_{nk} \end{bmatrix}, \quad \boldsymbol{\beta} = \begin{bmatrix} \beta_0 \\ \beta_1 \\ \vdots \\ \beta_n \end{bmatrix}, \quad \boldsymbol{\varepsilon} = \begin{bmatrix} \varepsilon_1 \\ \varepsilon_2 \\ \vdots \\ \varepsilon_n \end{bmatrix} \tag{3}$$

In the relation (3) $\boldsymbol{y}$ is an $(n \times 1)$ vector of the observations, $\boldsymbol{X}$ is an $(n \times p)$ matrix of the levels of the independent variables, $\boldsymbol{\beta}$ is a $(p \times 1)$ vector of the regression coefficients, and $\boldsymbol{\varepsilon}$ is an $(n \times 1)$ vector of random errors.

The fitted equation will be instead:

$$\hat{\boldsymbol{y}} = \boldsymbol{X}\hat{\boldsymbol{\beta}} \tag{4}$$

Where:

$$\hat{\boldsymbol{y}} = \begin{bmatrix} \hat{y}_1 \\ \hat{y}_2 \\ \vdots \\ \hat{y}_n \end{bmatrix}, \quad \boldsymbol{X} = \begin{bmatrix} 1 & x_{11} & x_{12} & \cdots & x_{1k} \\ 1 & x_{21} & x_{22} & \cdots & x_{2k} \\ \vdots & \vdots & \vdots & \ddots & \vdots \\ 1 & x_{n1} & x_{n2} & \cdots & x_{nk} \end{bmatrix}, \quad \hat{\boldsymbol{\beta}} = \begin{bmatrix} \hat{\beta}_0 \\ \hat{\beta}_1 \\ \vdots \\ \hat{\beta}_n \end{bmatrix} \tag{5}$$

In the relation (5) $\hat{\boldsymbol{y}}$ is a $(n \times 1)$ vector of the responses, $\boldsymbol{X}$ is an $(n \times p)$ matrix of the levels of the independent variables and $\hat{\boldsymbol{\beta}}$ is a $(p \times 1)$ vector of the estimated regression coefficient.

The residuals of the fitted model will be estimated as:

$$\boldsymbol{e} = \boldsymbol{y} - \hat{\boldsymbol{y}} \tag{6}$$

This modelling approach relies on two main hypothesis:

- The residuals of the model are normal, with mean $\mu = 0$;
- The residuals of the model follow a random pattern.

If one of these two hypothesis is rejected the model is not valid.

Alg+Gel

Regression model

The modelling started from the data gathered from the experiment with the Alg+Gel bioink.

Once uploaded on Minitab and reorganized according to their factors, the data regarding the Alg+Gel bioink were plotted in an Individual Value Plot grouped by pressure and velocity (Figure 27).

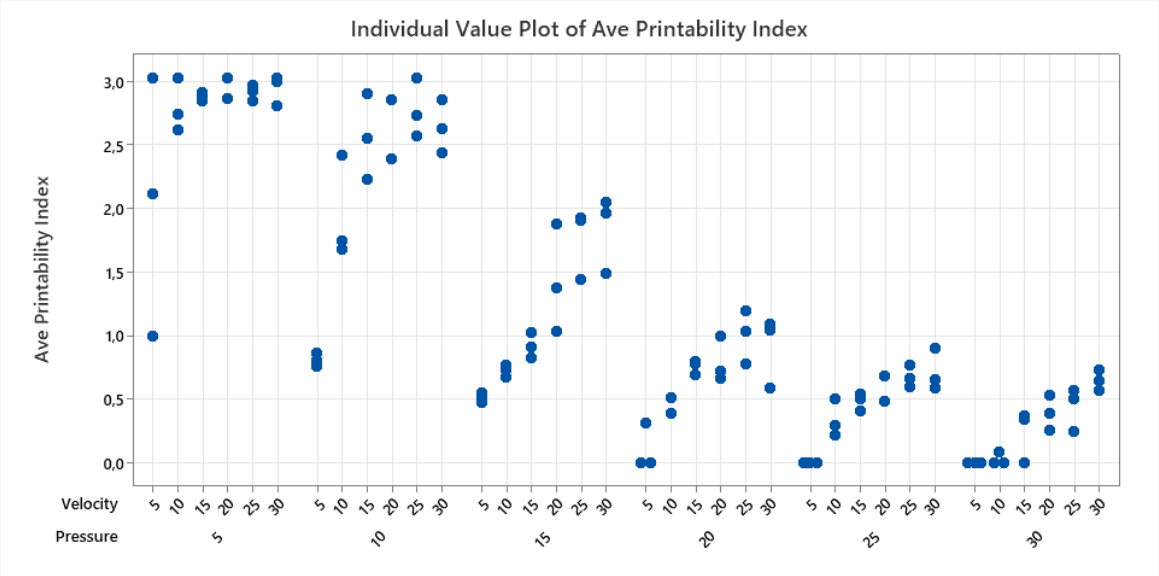

Figure 27: Individual Value Plot of API from Alg+Gel experimentation.

From the visualization of the individual values was possible to make the first observations.

Firstly, the data followed a clear pattern. Fixing the pressures, the API ranged from smaller values at low velocities, to larger values at high velocities. In fact, since the velocity impacts on the travelled distance of the printhead, if it makes a short travel at constant pressure, a larger amount of material will be deposited, shifting toward the over extrusion case with low API.

In the other hand, fixing the velocity, the values of API ranged from smaller values at high pressure, to higher values at low pressure. This reflects that at constant travelled distance, if the pressure increases the flow rate will increase as well, shifting towards the over extrusion case with low API.

Additionally, it was observed that many of the measured data reached the saturation values, both at the upper and lower saturation limit. In particular, almost all the data gathered at $P = 5$ fell in the upper saturation value.

From these observations the regression model was derived. To do so, as first step all the data corresponding to $P = 5$ were removed since did not represent the real variance of the phenomena. As regressors of the model were used Pressure (P) and Velocity (v) at the first order, together with all the second order interactions, namely $P * P$, $P * v$ and $v * v$.

From these assumptions was produced a preliminary model. The resulting model ($R^2\ adjusted = 91.39\%$) was used to identify the possible outliers with the module of the standardized residual higher than 2.9 ($|SRes| > 2.9$). Two observations were individuated as outlier and removed from the dataset ($n = 77;\ n = 100$).

Afterwards, with the new dataset containing 88 observations the definitive regression model equation was fitted (7).

Table 3: Model summary of the model Alg+Gel.

S	R-sq	R-sq(adj)
0.215200	93.26%	92.85%

$$API = 2.541 - 0.2518\,\boldsymbol{P} + 0.1460\,\boldsymbol{v} + 0.005186\,\boldsymbol{P} * \boldsymbol{P} - 0.001513\,\boldsymbol{v} * \boldsymbol{v} - 0.002487\,\boldsymbol{P} * \boldsymbol{v} \quad (7)$$

Table 4: Tests statistics on the coefficients of the model Alg+Gel.

Term	Coef	P-Value
Constant	2.541	0.000
Pressure	-0.2518	0.000
Velocity	0.1460	0.000
Pressure*Pressure	0.005186	0.000
Velocity*Velocity	-0.001513	0.000
Pressure*Velocity	-0.002487	0.000

The standardized residuals were then analyzed to verify the model's hypothesis. The normality test resulted in $P\text{-}value = 0.054$, while from the analysis of the Autocorrelation Function did not emerge any critical value (Appendix 7; Appendix 8).

Therefore, due to the test statistics on the regressors (Table 4), a to the not rejection of the hypothesis, the model was considered valid and significant.

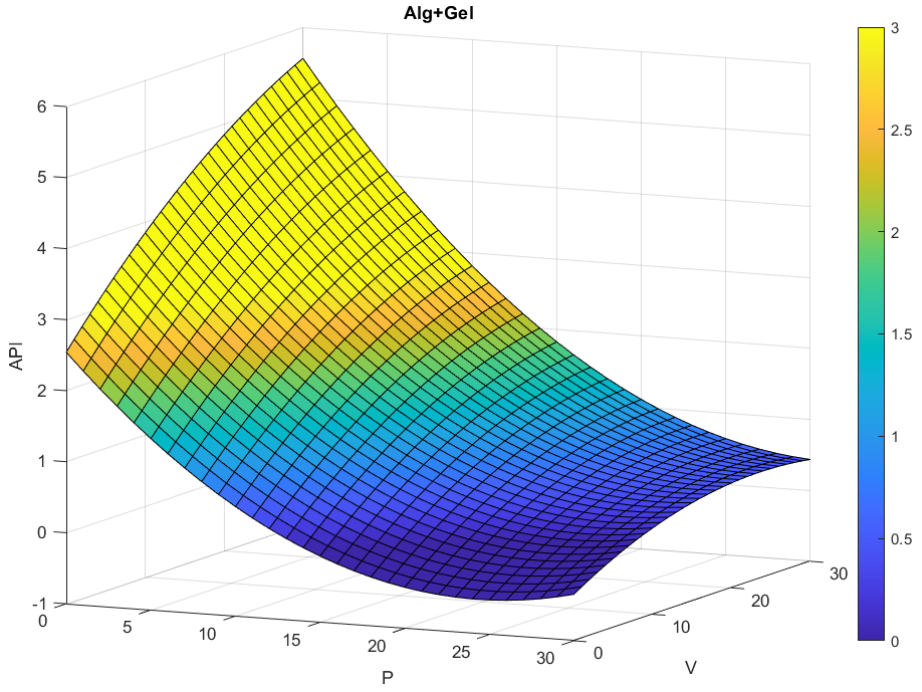

Figure 28: 3D plot of the fitted regression model of the Alg+Gel bioink.

The 3D plot of figure 28 represents the fitted regression model following the relation (4) with the vectors:

$$\boldsymbol{X} = \begin{bmatrix} 1 \\ P \\ v \\ P * P \\ v * v \\ P * v \end{bmatrix}, \qquad \widehat{\boldsymbol{\beta}} = \begin{bmatrix} 2.541 \\ -0.2518 \\ 0.1460 \\ 0.005186 \\ -0.001513 \\ -0.002487 \end{bmatrix}$$

Probability map

Once the model is fitted, it is possible to estimate the map of probability that an observation falls in the optimal interval of $API = [0.75\,;\,1.25]$. With the probability maps are considered both the prediction gathered from the model and the intrinsic uncertainty of the produced model. The prediction of the model, in fact, does not provide any information on the goodness of the prediction generated by itself. Probability maps, instead, represent a reliable tool that

integrates the importance of the prediction uncertainty contained in the regression model.

In order to estimate the probability map of the optimal interval, it is necessary to estimate the prediction uncertainty of the regression model in all the domain of the factors P and v. To do so, we have to identify $\Delta(\boldsymbol{x})$:

$$\Delta(\boldsymbol{x}) = \sqrt{MS_E(1 + \boldsymbol{x}^T(\boldsymbol{X}^T\boldsymbol{X})^{-1}\boldsymbol{x})}$$

(8)

We can plot the map of $\Delta(\boldsymbol{x})$ that identifies the regions with high and low prediction uncertainty.

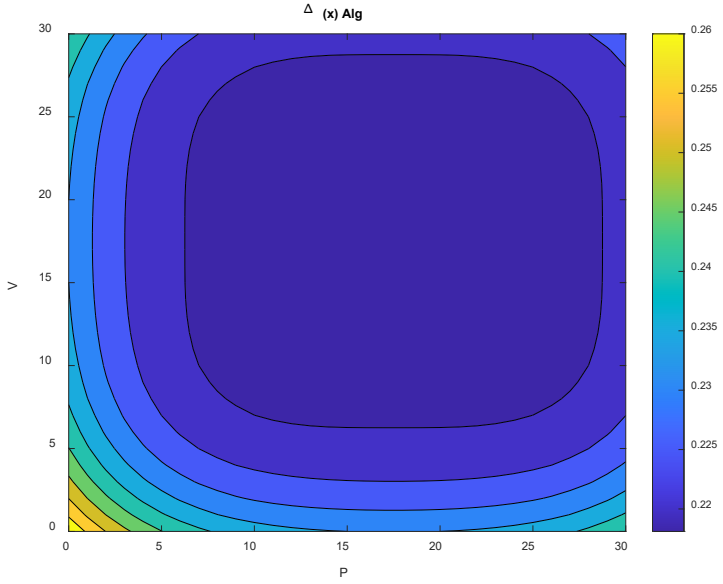

Figure 29: Colormap of the prediction uncertainty.

Now, in order to identify the probability of belonging to a certain interval, the following relation has to be solved:

$$P\{\alpha_{inf} \leq y(\boldsymbol{x}) \leq \alpha_{sup}\} \geq 1 - \alpha$$

(9)

This relation identifies the probability $P \geq 1 - \alpha$ of falling in the optimal interval $API = [0.75\ ;\ 1.25]$ — where $\alpha_{inf} = 0.75$ and $\alpha_{sup} = 1.25$ — based on the prediction of the observation $y(\boldsymbol{x})$.

Resolving the relation (9) introducing the prediction uncertainty term $\Delta(\boldsymbol{x})$:

$$F_{T,df_E}\left(\frac{\alpha_{sup} - \hat{y}(\boldsymbol{x})}{\Delta(\boldsymbol{x})}\right) - F_{T,df_E}\left(\frac{\alpha_{inf} - \hat{y}(\boldsymbol{x})}{\Delta(\boldsymbol{x})}\right) = 1 - \alpha \qquad (10)$$

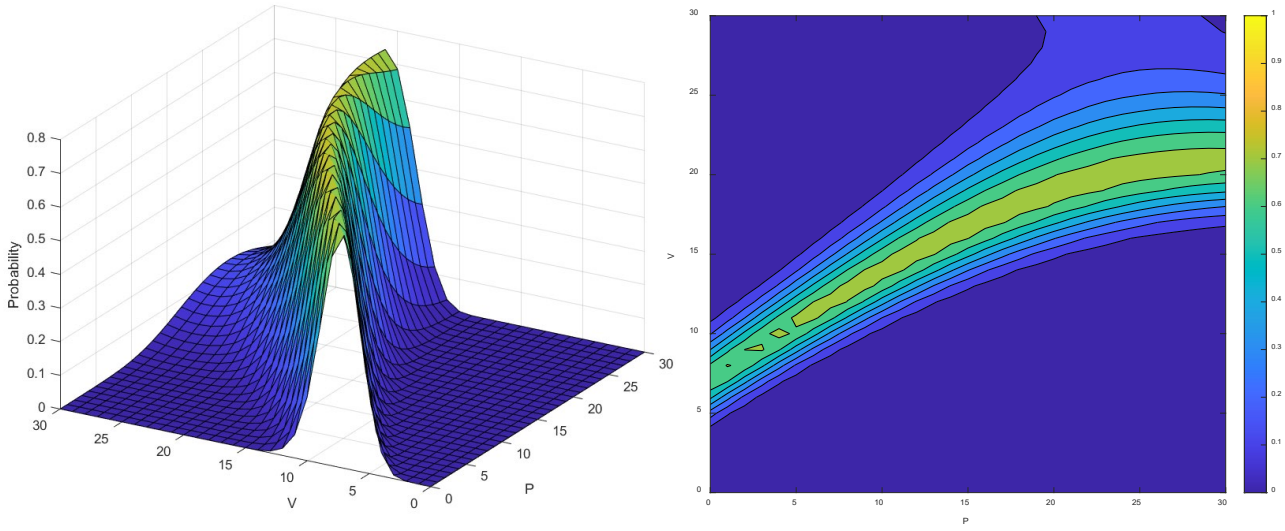

Figure 30: 3D surface plot and colormap of the Probability Map of Alg+Gel.

Figure 30 represents the probabilities of the relation (10) plotted in the examined domain of the factors P and v.

Alg

Regression model

The collected data regarding Alg were reorganized as well on Minitab and the individual value plot was generated (Figure 31).

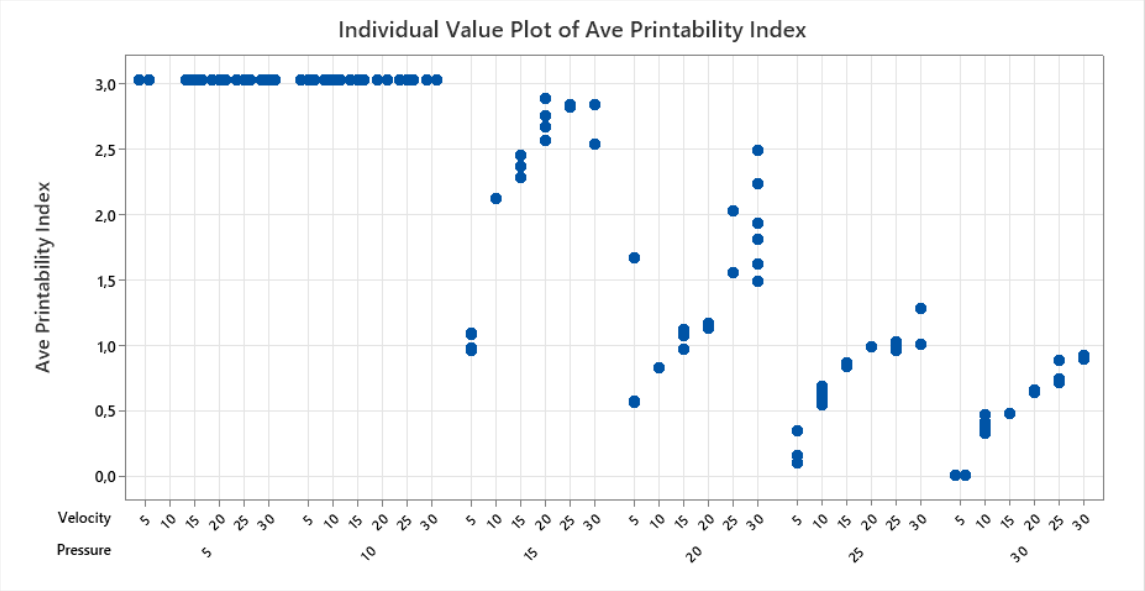

Figure 31: Individual Value Plot of API from Alg experimentation

It is immediately noticeable from the individual value plot the categorical failure of extrusion at low pressures. This behavior was observed also during the experimentations, since at pressures $P = 5$ and $P = 10$ the rheology of the bioink did not allow any extrusion. The result was that all the pictures gathered from the HD camera were empty, and consequently the image analysis algorithm provided the critical values of under extrusion for all those images. Regarding the data with a pressure greater than 10 the behavior was the same as in the case of Alg+Gel. The same modelling approach was therefore followed.

Firstly, all the data regarding the case of $P = 5$ and $P = 10$ were removed from the dataset since did not reflect the real variability of the phenomena. From the remaining data was then fitted the model. As for the case of Alg+Gel, a preliminary model was gathered to identify the outliers and remove them. From this model ($R^2\ adjusted = 90.06\%$) was removed the observation $n = 41$ and refitted the model (11).

Table 5: Model summary of the model Alg.

S	R-sq	R-sq(adj)
0.216217	93.58%	93.09%

$$API = 4.914 - 0.4049\,\boldsymbol{P} + 0.1810\,\boldsymbol{v} + 0.00773\,\boldsymbol{P}*\boldsymbol{P} - 0.001748\,\boldsymbol{v}*\boldsymbol{v} - 0.003180\,\boldsymbol{P}*\boldsymbol{v} \quad (11)$$

Table 6: Tests statistics on the coefficients of the model Alg.

Term	Coef	P-Value
Constant	4.914	0.000
Pressure	-0.4049	0.000
Velocity	0.1810	0.000
Pressure*Pressure	0.00773	0.000
Velocity*Velocity	-0.001748	0.000
Pressure*Velocity	-0.003180	0.000

Eventually, the residuals were analyzed. The residuals followed a normal distribution ($P\text{-}value = 0.706$) and did not present any autocorrelation function value out of control (Appendix 9; Appendix 10).

Therefore, due to the regressors significance, and due to the non-rejection of the hypothesis, the model was considered valid and significant.

The 3D plot of figure 32 displays the regression model following the relation (4), with:

$$\boldsymbol{X} = \begin{bmatrix} 1 \\ P \\ v \\ P*P \\ v*v \\ P*v \end{bmatrix}, \qquad \widehat{\boldsymbol{\beta}} = \begin{bmatrix} 4.914 \\ -0.4049 \\ 0.1810 \\ 0.00773 \\ -0.001748 \\ -0.003180 \end{bmatrix}$$

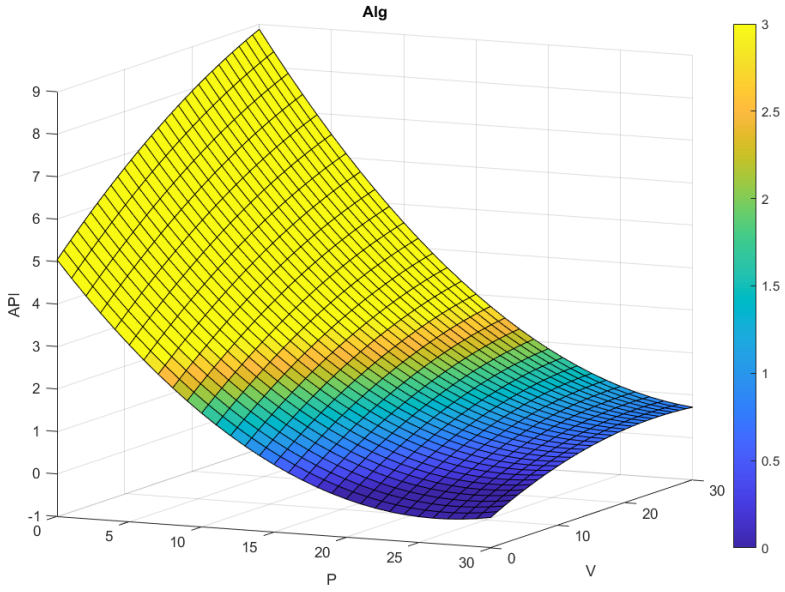

Figure 32: 3D plot of the fitted regression model of the Alg bioink.

Probability map

As for the case of Alg+Gel, it was firstly evaluated the map of $\Delta(\boldsymbol{x})$ to identify the prediction uncertainty, and secondly this result was integrated with the fitted model equation following the relation (10).

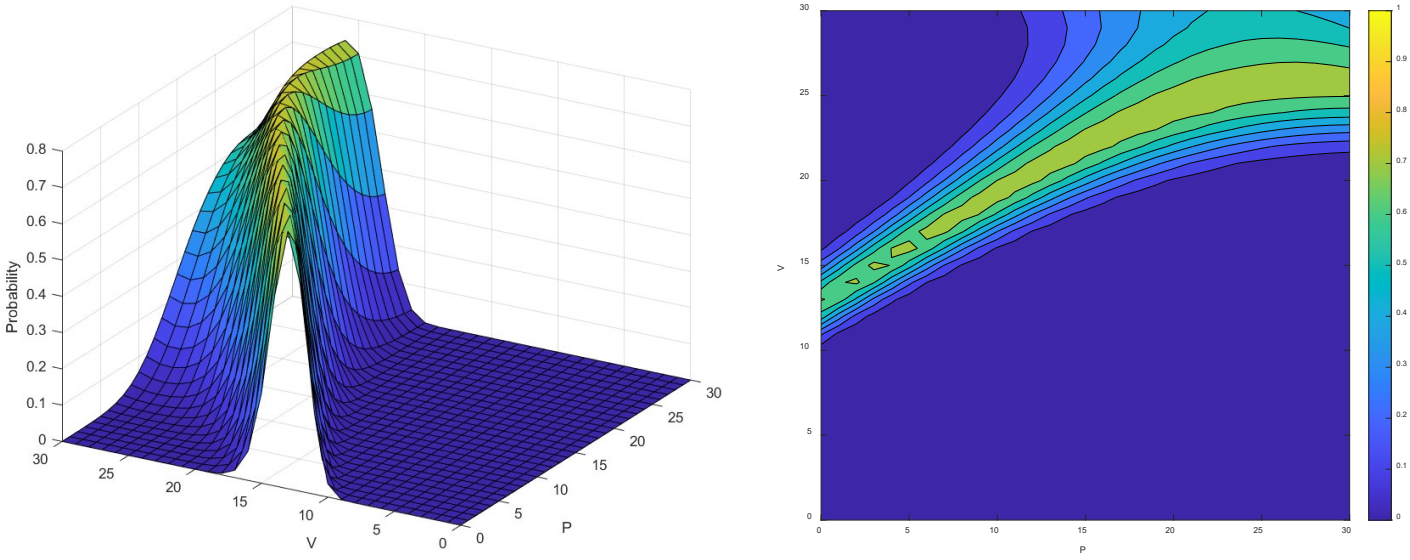

Figure 33: 3D surface plot and colormap of the Probability Map of Alg.

Conclusions

This thesis aimed at exploring the printability of two edible bioinks that can be implemented in CM applications. The work started with the identification of the suitable inks from an extensive literature review, which eventually ended in the identification of the formulations Alg and Alg+Gel. An experiment was then designed to assess the printability of these bioinks, in order to collect a dataset, and make a comprehensive data analysis of the results. With these results was possible to derive the regression models and the probability maps of the bioinks.

Identifying the regression equation of a model is a key step for the comprehension of the phenomena under analysis. In fact, once regressors are identified, it is possible to understand what variables are mostly impacting the response variable. This is a key aspect to have a fully understanding and control of a process.

As previously discussed, the modelling procedure followed was the same for both the bioinks. In fact — as noted during the experimentation and confirmed thanks to the visualization of the collected data of the two datasets — it was observed that the two bioinks followed the same behavior, but with a bias represented by the fact that the Alg bioink did not extrude at low pressures, while Alg+Gel did.

This behavior was then confirmed by the modelling. The two models were not fitted similarly in a forced way, as they both resulted to be very significant, with $R^2\ adjusted > 90\%$ and with the regressors' $P\text{-}values = 0$. In table 7 are collected the two regression model outputs.

Table 7: Comparison of the Alg+Gel and Alg model regressors.

Term	**β Alg+Gel**	**β Alg**
Constant	2.541	4.914
Pressure	-0.2518	-0.4049
Velocity	0.1460	0.1810
Pressure*Pressure	0.005186	0.00773
Velocity*Velocity	-0.001513	-0.001748
Pressure*Velocity	-0.002487	-0.003180

The two models have all the regression terms very similar to each other, with exception for the significant difference in the constant term. This means that the models are defining the same behavior, but with a bias determined by the rheology of the bioink. In fact, the proportional constant term of the Alg model is double the constant of the Alg+Gel model, reflecting the general under extrusion observed during the experimentation with pure alginate. The difference in the rheology can be also the reason in the smaller difference between the P terms of the models. In fact, the rheology directly impacts the pressure necessary for their extrusion, rather than the velocity of deposition.

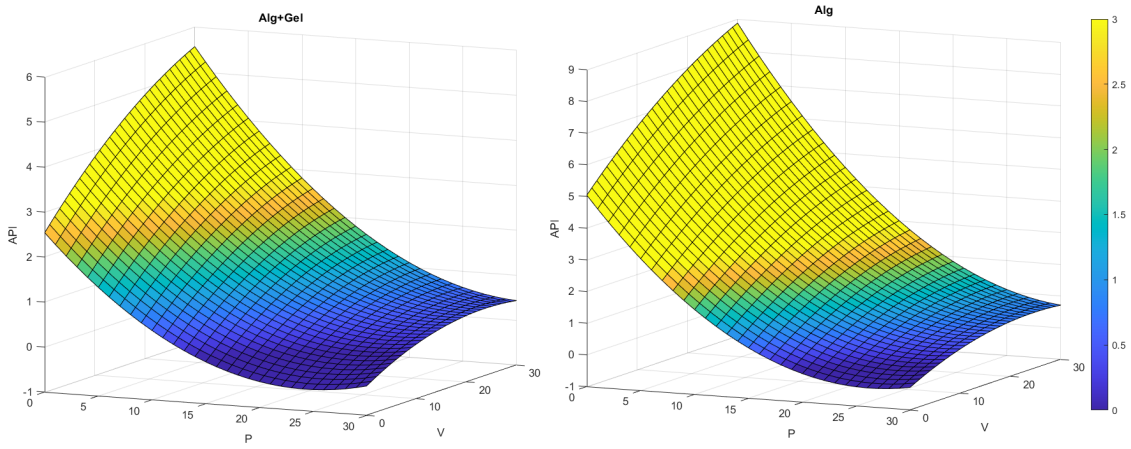

Figure 34: Comparison of the Alg+Gel and Alg model models surface plot.

Concerning the probability maps additional conclusions can be done. Probability maps, in fact, do not only provide the comprehension of the process behavior and influences, but opens the doors to the process optimization.

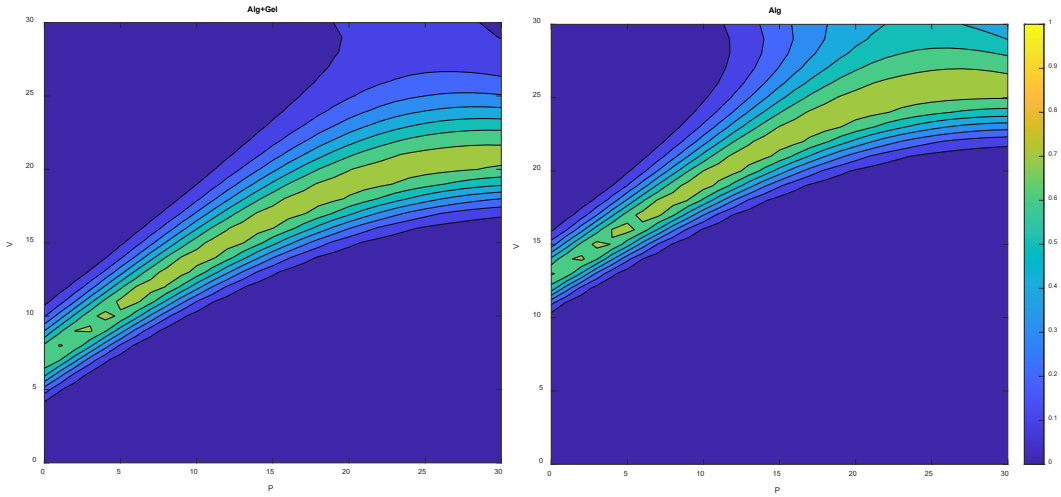

Figure 35: Comparison of the probability maps of Alg+Gel (on the left) and Alg (on the right).

The probability maps are indeed an important indicator of the process quality. They identify the operating regions where the final quality of the print is the closest to the optimal situation where $API = 1$ considering the uncertainties introduced by the model itself, process and measurement systems variability. In fact, with these probability maps, it was identified the region with highest probability to get a final quality in control between the upper and lower control limits $UCL = 1.25$ and $LCL = 0.75$.

It is therefore possible to fix a certain value of pressure or velocity, and consequently define an optimal operating region for the other. The fixed values can be identified by some process constraints — like the maximum operating pressure without harming the cells, or the lowest processing velocity to not make the process too long and dangerous for cells — or by optimization procedures. Optimization procedures are the key enablers to the goal of cost parity by 2035

cited in the work Witte et al.. In fact, CM is still far away from its market entry due to its high costs of processing. This product still needs optimized and cheap processing practices, that can be reached only by the optimization of the current technologies involved in its production.

The optimization can be pursued focusing on different aspects of the process. Firstly, the results of the probability map can be used to identify the optimal pressure of operation in order to minimize the time of printing. In fact, if we fix the velocity as high as possible, respecting the process constraints, it will be possible to identify the operating pressure interval that achieves the best printing conditions. Therefore, this will achieve the reduction in processing time, and consequently a cost reduction. The reduction of processing time will also affect the cellular activity: in fact, the longer cells are kept in a "open" environment without growth media, and the lower will be the final viability of the cellular population.

An alternative is to identify the energy consumption function that links pressure and velocity, and together with the probability map resolve a minimization problem to achieve minimal energy use. This is another important aspect to consider in order to access the scalability of this process. Energy optimization is a fundamental step in the cost reduction of the process. In fact, as for the previous case, this type of optimization will consequently impact the cost of processing due to reduce the cost of energy depletion.

Eventually, the model can be used to achieve the highest robustness and identify the optimal conditions for the quality reliability. In fact, pressure is a parameter that can suffer from fluctuations during the processing, while velocity is more stable and controllable. If we focus on robustness, it is possible to fix the velocity or pressure that identifies the widest region of high probability on the map. In

fact, if in the case of Alg on the right of figure 35 if the two values of velocity $v = 15$ and $v = 25\, mm/s$ are compared, it is immediately possible to see that the ranges of working pressure are very different (Figure 36). In the first case very few values of pressure are usable to achieve a good quality, while in the second case a much larger region of suitable pressures is identified. As result, adopting a velocity of $v = 25$ even in case of fluctuations in the pressure of extrusion, the quality of the print will not be significantly impacted.

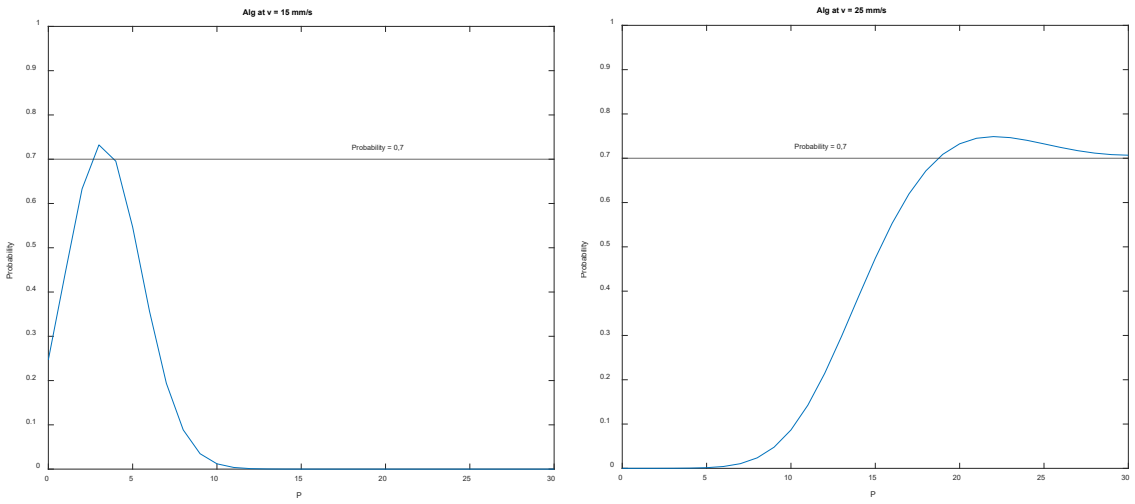

Figure 36: Comparison of the P intervals for high quality at *v=15 mm/s* and *v=25mm/s* in the Alg model.

Another important conclusion that can be done is on the similarity of the models. These models in fact have the same regressors but different vectors β of the proportional constants. This information can be interpreted as all the alginate based bioinks follow the same functional dependence to the variables P and v. In this way, any further exploration of printability of a new bioink with alginate as base will start with this regressors and find the proportionality constants from it. This will impact the design of experiment of further examinations, that will take as starting point the regression model structure used in this work.

Future development

As discussed in the introduction about process monitoring, the data analysis and model regression can be adopted in the formulation of closed-loop controllers. With these results, the implementation of the process controller will just need the identification of a closed-loop controller algorithm. In fact, the measuring unit would be an HD camera as the one used for this thesis, and the actuators are the same used by the bioprinter to set manually the process variables. Putting them in communication with either a P, PI or PID controller will then close the loop and create a control system integrated into the machine. This can be used to detect the over or under extrusion during the processing and correct it in in-situ to minimize the defected objects.

An additional development of this work could be the analysis of the influence of the nozzle temperature on the printability index. In this work the temperature was kept constant at 22°C, but for different bioink which are more heat-sensible (typically the polysaccharides) the temperature can be explored as an additional factor in the factorial experimentation. This could lead to the identification of the optimal temperature for the energy consumption minimization, or either to understand which temperature and velocity guarantee the wider pressure interval that for a probable high quality.

Another future development may be represented by the analysis of two additional dimensions: the Filament Fusion, and the Diameter Expansion. These additional parameters are two important features to consider for 3DBP for CM. In fact, the 3D for the analysis of PI was designed in order to measure these two dimension as well, however in this thesis the focus was given only to PI.

Filament Fusion accounts for the fusion of parallel filaments that are deposited adjacent to each other. This is an important feature to explore particularly for cultured meat applications, since in order to resemble the fibrous texture of meat, it is often bioprinted with parallel adjacent filaments, rather than rectangular or quadratic patterns typical of the biomedical 3DBP.

In the other hand, the Diameter Expansion refers to the final diameter of the extruded filament. This dimension intends to quantify the expansion or collapse of the filament after being extruded, that reaches a diameter larger than the diameter of the nozzle. This is another important measure because it influences both the Filament Fusion and the Printability Index. In fact, the greater will be the expansion of the diameter after extrusion, and the lower will be the printability index, and the higher will be the fusion of the adjacent filaments.

The development of these analysis can start from the images already collected for this thesis or can either start from a new design of experiment.

Extending this research to multi-layer case would be another important aspect of research. In this work were explored geometries only in two dimensions, while their assessment can be extended to the third dimension. This includes for example the evolution of certain variables along the z-axis. Additionally, the analysis of dimensions in the z direction introduces the evaluation of additional parameters, like the collapse of the filament along the "bridges" (when the bioink is deposited over distanced filaments, instead of being laid upon a continuous substrate), or the overall structural resistance of the construct.

Finally, this type of work can be extended to any type of bioink, combined with any of the extrusion-based machine configurations, which can be either with needles instead of nozzles, printing in cross-linking agent baths, or printing with different nozzle diameters. In particular are interesting the development of

animal-free ingredients bioinks, a key aspect for CM to be a definitive substitute of livestock meat. Additionally, this does not only apply to CM applications, but also to bioinks aimed to be used in biomedical applications, where measures like the filament fusion loose interest, but other like the printability index gains crucial importance for the resulting quality and mechanical resistance.

In fact, the potentiality of this type of work lays in the possibility to adapt it to the specific technology and identify the optimal quality regions characteristic of the case.

Bibliography

Asem-Hiablie, S., Battagliese, T., Stackhouse-Lawson, K. R., & Rotz, & C. A. (2018). *A life cycle assessment of the environmental impacts of a beef system in the USA*. https://doi.org/10.1007/s11367-018-1464-6

Bidarra, S. J., Barrias, C. C., Fonseca, K. B., Barbosa, M. A., Soares, R. A., & Granja, P. L. (2011). Injectable in situ crosslinkable RGD-modified alginate matrix for endothelial cells delivery. *Biomaterials*, *32*(31), 7897–7904. https://doi.org/10.1016/J.BIOMATERIALS.2011.07.013

Bodiou, V., Post, M. J., Moutsatsou, P., Knorr, D., & Tzanakakis, E. S. (2020). Microcarriers for Upscaling Cultured Meat Production. *Frontiers in Nutrition | Www.Frontiersin.Org*, *7*(10). https://doi.org/10.3389/fnut.2020.00010

Bomkamp, C., Skaalure, S. C., Fernando, G. F., Ben-Arye, T., Swartz, E. W., & Specht, E. A. (2021). *Scaffolding Biomaterials for 3D Cultivated Meat: Prospects and Challenges*. https://doi.org/10.1002/advs.202102908

Boularaoui, S., Al Hussein, G., Khan, K. A., Christoforou, N., & Stefanini, C. (2020). An overview of extrusion-based bioprinting with a focus on induced shear stress and its effect on cell viability. *Bioprinting*, *20*. https://doi.org/10.1016/j.bprint.2020.e00093

Bugatti, M., & Colosimo, B. M. (2022). Towards real-time in-situ monitoring of hot-spot defects in L-PBF: a new classification-based method for fast video-imaging data analysis. *Journal of Intelligent Manufacturing*, *33*(1), 293–309. https://doi.org/10.1007/S10845-021-01787-Y/TABLES/5

Caló, E., & Khutoryanskiy, V. V. (2015). Biomedical applications of hydrogels: A review of patents and commercial products. *European Polymer Journal*, *65*, 252–267. https://doi.org/10.1016/J.EURPOLYMJ.2014.11.024

Colosimo, B. M., Huang, Q., Dasgupta, T., & Tsung, F. (2018). Opportunities and challenges of quality engineering for additive manufacturing. *Journal of Quality Technology*, *50*(3), 233–252. https://doi.org/10.1080/00224065.2018.1487726

Derakhshanfar, S., Mbeleck, R., Xu, K., Zhang, X., Zhong, W., & Xing, M. (2018). 3D bioprinting for biomedical devices and tissue engineering: A review of recent trends and advances. *Bioactive Materials*, *3*(2), 144–156. https://doi.org/10.1016/J.BIOACTMAT.2017.11.008

Dutta, S. D., Ganguly, K., Jeong, M.-S., Patel, D. K., Patil, T. V., Cho, S.-J., & Lim, K.-T. (2022). Bioengineered Lab-Grown Meat-like Constructs through 3D Bioprinting of Antioxidative Protein Hydrolysates. *ACS Applied Materials & Interfaces*, *14*(30), 34513–34526. https://doi.org/10.1021/ACSAMI.2C10620

Everton, S. K., Hirsch, M., Stavroulakis, P. I., Leach, R. K., & Clare, A. T. (2016). Review of in-situ process monitoring and in-situ metrology for metal additive manufacturing. *Materials and Design*, *95*, 431–445. https://doi.org/10.1016/J.MATDES.2016.01.099

Ferroni, L., Albini, E., Lovito, C., Blasi, F., Maresca, C., Massacci, F. R., Orsini, S., Tofani, S., Pezzotti, G., Diaz Vicuna, E., Forte, C., & Magistrali, C. F. (2022). Antibiotic consumption is a major driver of antibiotic resistance in calves raised on Italian cow-calf beef farms. *Research in Veterinary Science*, *145*, 71–81. https://doi.org/10.1016/J.RVSC.2022.01.010

Fima, S., Gal, I., & MEATECH 3D. (2020). *CULTURED EDIBLE MEAT FABRICATION USING BIO-PRINTING*.

Gaillac, R., & Marbach, S. (2021). The carbon footprint of meat and dairy proteins: A practical perspective to guide low carbon footprint dietary choices. *Journal of Cleaner Production*, *321*. https://doi.org/10.1016/J.JCLEPRO.2021.128766

Grasso, M., & Colosimo, B. M. (2017). Process defects and in situ monitorin1. Grasso M, Colosimo BM. Process defects and in situ monitoring methods in metal powder bed fusion: A review. Meas Sci Technol. 2017 Apr 1;28(4). g methods in metal powder bed fusion: A review. *Measurement Science and Technology*, *28*(4). https://doi.org/10.1088/1361-6501/AA5C4F

Hölzl, K., Lin, S., Tytgat, L., Van Vlierberghe, S., Gu, L., & Ovsianikov, A. (2016). Bioink properties before, during and after 3D bioprinting. *Biofabrication*, *8*, 32002. https://doi.org/10.1088/1758-5090/8/3/032002

Ianovici, I., Zagury, Y., Redenski, I., Lavon, N., & Levenberg, S. (2022). 3D-printable plant protein-enriched scaffolds for cultivated meat development. *Biomaterials*, *284*, 121487. https://doi.org/10.1016/J.BIOMATERIALS.2022.121487

Ilea, R. C. (2008). *Intensive Livestock Farming: Global Trends, Increased Environmental Concerns, and Ethical Solutions*. 15. https://doi.org/10.1007/s10806-008-9136-3

Jo, B., Nie, M., & Takeuchi, S. (2021). Manufacturing of animal products by the assembly of microfabricated tissues. *Essays in Biochemistry*, *65*, 611–623. https://doi.org/10.1042/EBC20200092

K. Handral, H., Hua Tay, S., Wan Chan, W., & Choudhury, D. (2020). 3D Printing of cultured meat products. *Https://Doi.Org/10.1080/10408398.2020.1815172*, *62*(1), 272–281. https://doi.org/10.1080/10408398.2020.1815172

K. Handral, H., Hua Tay, S., Wan Chan, W., & Choudhury, D. (2022). 3D Printing of cultured meat products. *Critical Reviews in Food Science and Nutrition*, *62*(1), 272–281. https://doi.org/10.1080/10408398.2020.1815172

Kang, D.-H., Louis, F., Liu, H., Shimoda, H., Nishiyama, Y., Nozawa, H., Kakitani, M., Takagi, D., Kasa, D., Nagamori, E., Irie, S., Kitano, S., & Matsusaki, M. (2021). *Engineered whole cut meat-like tissue by the assembly of cell fibers using tendon-gel integrated bioprinting*. https://doi.org/10.1038/s41467-021-25236-9

Lanzoni, D., Bracco, F., Cheli, F., Colosimo, B. M., Moscatelli, D., Baldi, A., Rebucci, R., & Giromin, C. (2022). *Biotechnological and Technical Challenges Related to CulturedMeat Production*. https://doi.org/10.3390/app12136771

Lee, J.-H., & Kim, H.-W. (2018). *Emerging properties of hydrogels in tissue engineering*. https://doi.org/10.1177/2041731418768285

Levi, S., Yen, F.-C., Baruch, L., & Machluf, M. (2022). Scaffolding technologies for the engineering of cultured meat: Towards a safe, sustainable, and scalable production. *Trends in Food Science & Technology*. https://doi.org/10.1016/J.TIFS.2022.05.011

Li, Y., Liu, W., Li, S., Zhang, M., Yang, F., & Wang, S. (2021). Porcine skeletal muscle tissue fabrication for cultured meat production using three-dimensional bioprinting technology. *Journal of Future Foods*, *1*(1), 88–97. https://doi.org/10.1016/J.JFUTFO.2021.09.005

Lindner, N., & Blaeser, A. (2022). Scalable Biofabrication: A Perspective on the Current State and Future Potentials of Process Automation in 3D-Bioprinting Applications. *Frontiers in Bioengineering and Biotechnology*, *10*. https://doi.org/10.3389/FBIOE.2022.855042

Montgomery, D. C. (2013). *Design and Analysis of Experiments*. https://books.google.it/books?hl=en&lr=&id=Py7bDgAAQBAJ&oi=fnd&pg=PA1&dq=design+and+analysis+of+experiments+montgomery&ots=X7v-t2SP35&sig=ldKg9bYCpFaxJSALUc-zbSx5uQw#v=onepage&q=design and analysis of experiments montgomery&f=false

Montgomery, D. C. (2019). Introduction to Statistical Quality Control, 8th Edition | Wiley. *Wiley Online Library*, 786. https://www.wiley.com/en-us/Introduction+to+Statistical+Quality+Control%2C+8th+Edition-p-9781119399308

Morach, B., Clausen, M., Rogg, J., Michael Brigl, Schulze, U., Nico Dehnert, Markus Hepp, Veronique Yang, Torsten Kurth, E. von K., Jens Burchardt, Björn Witte, Przemek Obloj, Sedef Koktenturk, F., Grosse-Holz, & Meinl, O. S.-N. (2022). *Food for Thought: The Untapped Climate Opportunity in Alternative Proteins | BCG*. https://www.bcg.com/publications/2022/combating-climate-crisis-with-alternative-protein

Moritz, M. S. M., Verbruggen, S. E. L., & Post, M. J. (2015). Alternatives for large-scale production of cultured beef: A review. *Journal of Integrative Agriculture*, *14*(2), 208–216. https://doi.org/10.1016/S2095-3119(14)60889-3

O'Riordan, K., Fotopoulou, A., & Stephens, N. (2017). The first bite: Imaginaries, promotional publics and the laboratory grown burger. *Public Understanding of Science*, *26*(2), 148–163. https://doi.org/10.1177/0963662516639001

Ouyang, L., Yao, R., Zhao, Y., & Sun, W. (2016). Effect of bioink properties on printability and cell viability for 3D bioplotting of embryonic stem cells. *Biofabrication*, *8*(3). https://doi.org/10.1088/1758-5090/8/3/035020

Paxton, N., Smolan, W., Böck, T., Melchels, F., Groll, J., & Jungst, T. (2017). *Proposal to assess printability of bioinks for extrusion-based bioprinting and evaluation of rheological properties governing bioprintability*. https://doi.org/10.1088/1758-5090/aa8dd8

Poore, J., & Nemecek, T. (2018). Reducing food's environmental impacts through producers and consumers. *Science*, *360*(6392), 987–992. https://doi.org/10.1126/SCIENCE.AAQ0216/SUPPL_FILE/AAQ0216_DATA S2.XLS

Sachlos, E., Czernuszka, J. T., Gogolewski, S., & Dalby, M. (2003). Making tissue engineering scaffolds work. Review on the application ofsolid freeform fabrication technology to the production of tissue engineeringscaffolds. *European Cells and Materials*, *5*, 29–40. https://doi.org/10.22203/ecm.v005a03

Santoni, S., Gugliandolo, S. G., Sponchioni, M., Moscatelli, D., & Colosimo, B. M. (2022). *3D bioprinting: current status and trends-a guide to the literature and industrial practice*. *5*, 14–42. https://doi.org/10.1007/s42242-021-00165-0

Schmieg, B., Gretzinger, S., Schuhmann, S., Guthausen, G., & Hubbuch, J. (2022). *Magnetic resonance imaging as a tool for quality control in extrusion-based*

bioprinting. https://doi.org/10.1002/biot.202100336

Seah, J. S. H., Singh, S., Tan, L. P., & Choudhury, D. (2021). Scaffolds for the manufacture of cultured meat. *Https://Doi.Org/10.1080/07388551.2021.1931803*, *42*(2), 311–323. https://doi.org/10.1080/07388551.2021.1931803

Springmann, M., Godfray, H. C. J., Rayner, M., & Scarborough, P. (2016). Analysis and valuation of the health and climate change cobenefits of dietary change. *Proceedings of the National Academy of Sciences of the United States of America*, *113*(15), 4146–4151. https://doi.org/10.1073/PNAS.1523119113/SUPPL_FILE/PNAS.1523119113.SAPP.PDF

Strauß, S., Schroth, B., & Hubbuch, J. (2022). Evaluation of the Reproducibility and Robustness of Extrusion-Based Bioprinting Processes Applying a Flow Sensor. *Frontiers in Bioengineering and Biotechnology*, *10*, 80. https://doi.org/10.3389/FBIOE.2022.831350/BIBTEX

Vijayavenkataraman, S., Yan, W. C., Lu, W. F., Wang, C. H., & Fuh, J. Y. H. (2018). 3D bioprinting of tissues and organs for regenerative medicine. *Advanced Drug Delivery Reviews*, *132*, 296–332. https://doi.org/10.1016/J.ADDR.2018.07.004

Wenger, L., Strauß, S., & Hubbuch, J. (2022). Automated and dynamic extrusion pressure adjustment based on real-time flow rate measurements for precise ink dispensing in 3D bioprinting. *Bioprinting*, *28*, e00229. https://doi.org/10.1016/J.BPRINT.2022.E00229

Witte, B., Obloj, P., Koktenturk, S., Morach, B., Brigl, M., Rogg, J., Schulze, U., Walker, D., Koeller, V., Dehnert, N., & Grosse-Holz, F. (2021). *Food for Thought The Protein Transformation*. www.bluehorizon.com.

Yang, W., Tu, A., Ma, Y., Li, Z., Xu, J., Lin, M., Zhang, K., Jing, L., Fu, C., Jiao, Y., & Huang, L. (2022). Chitosan and whey protein bio-inks for 3d and 4d printing applications with particular focus on food industry. *Molecules*, *27*(1). https://doi.org/10.3390/MOLECULES27010173

Zammit, P. S., Partridge, T. A., & Yablonka-Reuveni, Z. (2006). *The Skeletal Muscle Satellite Cell: The Stem Cell That Came in From the Cold*. https://doi.org/10.1369/jhc.6R6995.2006

Appendix

Appendix A.1: Patents analysis of the Cultured Meat companies listed on the Good Food Institute (Source: Good Food Institute).

COMPANY	TECHNOLOGY	PATENT	NOTES
3D BIO-TISSUES LTD.	Not Specified	NOVEL CORNEAL TISSUES AND METHODS OF MAKING THE SAME	Non Food Related. The proteins involved in the study are Collage, Lumican, Laminin and Fibronectin.
		COLLAGEN PRODUCTION	Process for production of collage. Focus on ETTS lipopeptides presence in the collagen.
ALEPH FARMS	Scaffolding	HIGH QUALITY CULTURED MEAT, COMPOSITIONS AND METHODS FOR PRODUCING SAME	Focus on the additives that enhance the perceived quality of the final product, such as vitamins, colorants, fatty acids, iron etc.
		3D-PRINTABLE PROTEIN-ENRICHED SCAFFOLDS	Patent that describes the materials and technology adopted in the production of 3D-printable scaffold. Follows the work described by Ianovici et al. (R&D responsible for Aleph Farms). Therefore, as for the article, no indication about cell density is provided, due to the absence of cell-laden bioink.
		CELL-FREE ANIMAL COLLAGEN, METHODS OF PRODUCTION AND USES THEREOF	Method to produce collagen matrix free of cells, using genetically modified cells.
		CULTIVATION SYSTEMS AND METHODS FOR LARGE-SCALE PRODUCTION OF CULTURED FOOD	Bio-reactor configuration and process scheme. Gives information on materials of the machinery, process control systems.

		CULTURED MEAT COMPOSITIONS	Describes the composition of the cell culture. In addition, gives information on the composition of the scaffold, but only referring to the presence of TSP (Textural Soy Proteins) and polysaccharides (generic indication, does not specify which one is used).
		PLURIPOTENT CELL AGGREGATES AND USE THEREOF	Describes a process that optimize the Pluripotent Stem Cells proliferation based on an aggregation and disaggregation in series approach.
ANTS INNOVATE	Not Specified	COLOUR CONTROL OF PLANT-BASED MEATS BY POLYPHENOL OXIDATION	Is not related to the company business but describes the use of an agent able to penetrate the cell membrane and change the color of alternative meat product. The materials are plant based.
ARTEMYS FOODS	Scaffolding	ANIMAL CELL LINES FOR FOODS CONTAINING CULTURED ANIMAL CELLS	Focus on cell RNA sequencing modification in order to achieve the desired differentiations for the final product. Also, the actual RNA sequence is cited and patented. One of the image describes the process with also the use of 3D printing, but it isn't described in the embodiment of the patent. They actually seed cells on pre-cooked plant based burger patties.
AVANT MEATS	Scaffolding	METHODS OF MEAT PRODUCTION BY IN VITRO CELL CULTIVATION	Focus on the RNA modification and cultivation of the fish cells in order to have a living line of muscular fish cells.
		QUANTIFICATION OF CELLS EMBEDDED IN A 3D SCAFFOLD	Method for dissolving a collagen scaffold and obtain a solution of cells to be counted in a live dead count.
		CELL HYDROLYSATE COMPOSITION FROM CULTIVATED CELLS AND APPLICATIONS THEREOF	Technology that uses cultured cells for growing hydrolysates (for many aims: skin care, food additives, wound care etc.) instead of the more traditional extraction of such compounds from plant and

			animal living beings. No specific food application.
BIFTEK	Production of FBS alternative	MICROBIOTA-DERIVED POSTBIOTICS: ALTERNATIVE SUPPLEMENT TO FETAL BOVINE SERUM FOR CULTURED MEAT	FBS alternative derived by microbial products.
BIOMIMETIC SOLUTIONS	Scaffolding	MATRICES FOR TISSUE ENGINEERING IN THE FORM OF FOAMS, FIBRES AND/OR MEMBRANES FORMED OF POLYMERS, CERAMICS, POLYMERIC COMPOSITES AND/OR CERAMIC COMPOSITES CONTAINING BIXA ORELLANA L. EXTRACT AND METHOD OF PRODUCTION	Materials and inner geometry of a scaffold for tissue engineering applications (not only food), composed mainly by ceramics and polymers. This scaffold is capable of tissue regeneration.
BIOTECH FOODS	Scaffolding	BIOREACTOR AND METHOD FOR THE PRODUCTION OF ADHERENT CELL CULTURES EMPLOYING SAID BIOREACTOR	Description of a bioreactor for the growth of seeded scaffolds. Description of geometry, components, and its working principle.
		METHOD FOR THE SYNTHESIS OF AN EDIBLE AND STERILIZABLE POROUS 3D SCAFFOLD SUITABLE FOR USE IN THE LARGE-SCALE PRODUCTION OF CULTURED MEAT	Description of the manufacturing of a porous scaffold composed preferably of alginate and/or chitosan. The scaffold also contains cell-adhesion additives (like RGD containing peptides) and cross linking agents. Describes the edibility of the materials as certificated by the EFSA and the US FDA. This work suggests to not work with gelatin, albumin, or

			other similar proteins because the hot steam sterilization would cause their denaturation.
		EDIBLE AND STERILIZABLE POROUS 3D SCAFFOLD AND USES THEREOF	Focus of the previous patent (METHOD FOR THE SYNTHESIS OF AN EDIBLE AND STERILIZABLE POROUS 3D SCAFFOLD SUITABLE FOR USE IN THE LARGE-SCALE PRODUCTION OF CULTURED MEAT) on the sterilizability of the scaffold, due to its composition.
		PROCESS AND DEVICE FOR PRODUCTION OF CULTURED MEAT	Description of the process of sterilizing the scaffold, seeding the cells, and putting the scaffold into the bioreactors.
CUBIQ FOODS	Emulsion of cells and water	STRUCTURED FAT SYSTEM WITH REDUCED CONTENT IN OR FREE FROM TRANS AND SATURATED FATTY ACIDS AND USES THEREOF FOR THE PREPARATION OF FOODSTUFFS	Production of an emulsion of fat and water emulsified with pea proteins. The fat cells are cultured, and a hydrocolloid as alginate, gelatin or similar polymers are used for the stabilization of the emulsion.
UPSIDE FOODS	Non-edible Scaffolding	METHOD FOR SCALABLE SKELETAL MUSCLE LINEAGE SPECIFICATION AND CULTIVATION	Focus on genetic modification of cells to enhance their differentiation rate.
		COMPOSITIONS AND METHODS FOR INCREASING THE EFFICIENCY OF CELL CULTURES USED FOR FOOD PRODUCTION	Focus on genetic modification of cells to enhance their differentiation rate ad culture density.
		NUTRIENT MEDIA FOR THE PRODUCTION OF SLAUGHTER-FREE MEAT	FBS alternative composed by a listed amino acids recipe.

		METHODS FOR EXTENDING THE REPLICATIVE CAPACITY OF SOMATIC CELLS DURING AN EX VIVO CULTIVATION PROCESS	Focus on genetic modification of cells to extend their replicative capacity.
		APPARATUSES AND METHODS FOR PREPARING A COMESTIBLE MEAT PRODUCT	Description of a substrate (solid and non-edible) and the carvings on its surface in order to maximize the cell growth. The final scaffold is made of a non-edible material that has to be removed.
		APPARATUSES AND SYSTEMS FOR PREPARING A MEAT PRODUCT	Description of the bioreactor configuration and positioning of the solid scaffold within it.
		SYSTEMS, DEVICES, AND METHODS FOR STERILIZING BIOREACTORS AND CULTURE MEDIA	Method for sterilizing the rotating bioreactor descripted in the patent "APPARATUSES AND SYSTEMS FOR PREPARING A MEAT PRODUCT".
		CHARACTERISTICS OF MEAT PRODUCTS	Description of the composition of the cultured meat that this company produces, with reference to specific amino acids, fatty acids, and the overall expected shelf life.
CYTONEST, INC	Scaffolding	METHODS AND DEVICES FOR MAKING NANOFIBERS AND NANOFIBER SCAFFOLDS	Description of the technique to produce scaffolds, consisting of depositing different droplets that form a filament during the free fall, that put together generate a fibrous scaffold. No indications about the material and its edibility.
FORK AND GOODE	Scaffolding; focus on scaling up	LARGE SCALE CELL CULTURE SYSTEM FOR MAKING MEAT AND ASSOCIATED PRODUCTS	Process configuration for the scaling up of cultured meat. The process scheme has different vessels for kidney, cardiac and skeletal cells, with a pump for circulating fresh medium and collecting the discharged medium.
		DRIED FOOD PRODUCTS FORMED FROM CULTURED MUSCLE CELLS	Description of the production of dried snack obtained by drying a thin layer of cultured cells mixed with Low Methyl (LM) Pectin.

GELATEX TECHNOLOGIES	Scaffolding providers	GELATIN-BASED NANOFIBROUS NON-WOVEN MATERIAL	Interesting cross-linking of gelatin with plasma radiations, or thermal treatment or electron beam irradiation. The whole process of cross-linking continues with a second step of physical cross linking with polymers, forming a covalent bond with the gelatin chains, and a further chemical cross-linking with cross-linking agents.
		DEVICE AND METHOD FOR PRODUCING POLYMER FIBERS AND ITS USES THEREOF	Machine and its configuration for producing fibrous scaffold, composed by a bio-based polymers.
HIGHER STEAKS	Scaffold	SYSTEMS AND METHODS FOR CELL CONVERSION	A degradable scaffold is described to dissolve at a rate of 1% during the culturing phase in bioreactors. The material list comprehends commonly used biomaterials like alginate, gelatin, fibrin, collagen, agar, cassava, chitosan, etc. with RGD-modified monomers. To give the typical meat texture are also used TVP (Texturized Vegetable Proteins) and flavorings.
MEATECH 3D	3D Bioprinting	PHYSICAL MANIPULATION OF CULTURED MUSCLE TISSUE	Gives information about the overall printing procedure, and the post processing in specific containers for the cell maturation.
		BIOPRINTER PRINT HEAD	Patent describing the Printer configuration and components from a Mechanical point of view.
		CULTURED EDIBLE MEAT FABRICATION USING BIO-PRINTING	Description of the process of cellular deposition. The bioprinter involved is multi-nozzle inkjet, where are deposited respectively a cell-laden bioink, a support substrate and a cross-linking agent in order to form a single layer.
MISSION BARNS	Scaffolding	SCALABLE BIOREACTOR SYSTEMS AND	Description of a scalable bioreactor that has a stack of mesh rotating within it, coated in a bio-

		RELATED METHODS OF USE	compatible edible material. The materials in the patent are not clear in their application, but some edible material is listed (mentioned often as carbohydrate-based or sugar-based material).
MOSA MEAT	Scaffolding	APPARATUS AND PROCESS FOR PRODUCTION OF TISSUE FROM CELLS	Structure of the plates holding the hydrogel, in an apparatus where these plates are stackable. This configuration is meant to be manually uploaded and later put in the incubator for the cell's differentiation. Non scalable approach. The material of the hydrogels is briefly described.
		SERUM-FREE MEDIUM FOR CULTURING A BOVINE PROGENITOR CELL.	Focus on FBS alternative
		PACKAGING OF CULTURED TISSUE	Method to pack the sterile cultured meat in such way that the final enclosure keeps its sterility. Focus on packaging for the final product.
		HYDROGELS FOR CULTURED MEAT PRODUCTION	Hydrogel composition, based on alginate coupled with RGD. Alginate of this patent has a low molecular weight, and the RGD is coupled via carbodiimide chemistry.
ORBILLION BIO	Microcarriers	USING ORGANOIDS AND/OR SPHEROIDS TO CULTIVATE MEAT	Method for producing spheroids composed by a scaffold and myocytes dispersed in it, used for the cell proliferation and differentiation. The material of the scaffold is not indicated.
SHIOK MEATS	Not Specified	ISOLATION AND CULTIVATION OF MUSCLE AND FAT CELLS FROM CRUSTACEANS	Generic description of the isolation and cultivation of cell derived from crustaceans. No indication of materials and technology of scaffolding.
SUPERMEATS	Hybrid	CULTURED MEAT-CONTAINING HYBRID FOOD	Food product composed by 80% of plant based ingredients, and the remaining by oils and fats, and cultured cells to enhance the meat texture and flavor. The cells do not form a tissue.

VITAL MEAT	Hybrid	AVIAN STEM CELLS FOR THE PRODUCTION OF A FOOD PRODUCT	Similar to the approach of SuperMeats, they produce a meat product mixing cultivated stem cells with food additives such as emulsifiers, thickeners etc.
WILD TYPE	Scaffolding	SYNTHETIC FOOD COMPOSITIONS	Definition of the production of cultured meat with a scaffold made of fibers. The scaffold is obtained through electro spinning, and the polymers listed in the patent are all edible.
		EX VIVO MEAT PRODUCTION	Similar to the other patent of the same company (SYNTHETIC FOOD COMPOSITIONS).

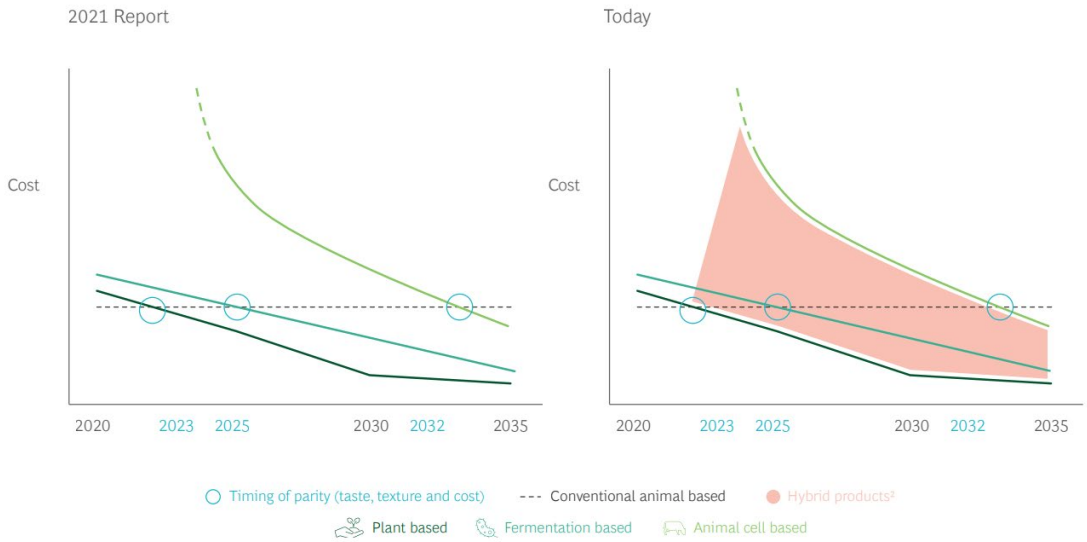

Appendix 2: Relative timing of cost parity for alternative proteins with taste and texture similar to conventional animal-based proteins (Source: Morach et al., 2022).

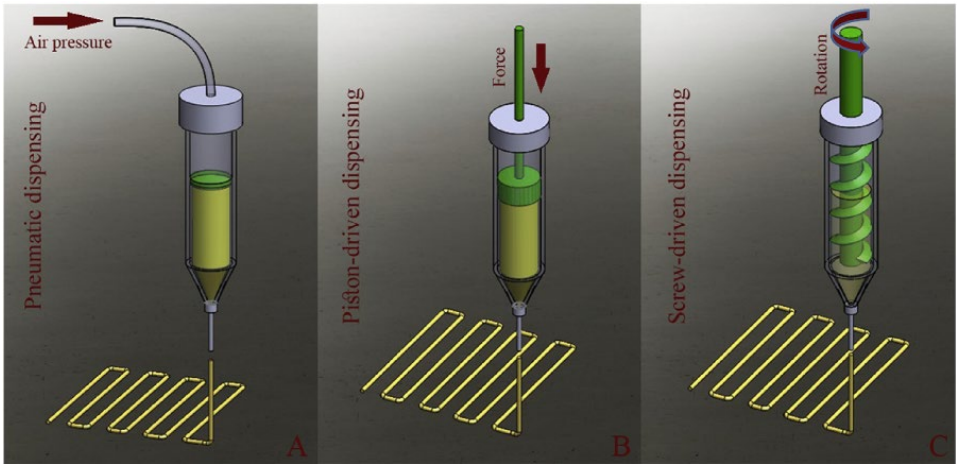

Appendix 3: Schematic diagram of: A) pneumatic B) piston C) screw-driven extrusion-based bioprinting extruders (Source: Derakhshanfar et al., 2018).

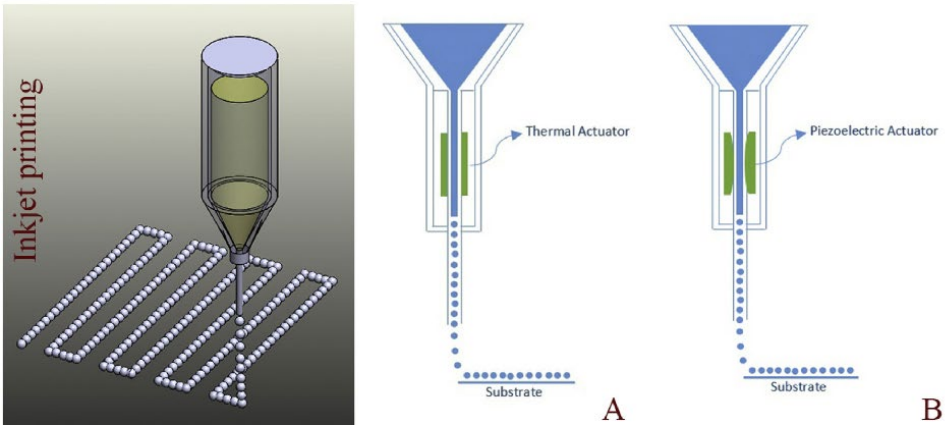

Appendix 4: Schematic diagram of drop-on-demand inkjet printing method using A) Thermal, and B) Piezoelectric actuators (Source: Derakhshanfar et al., 2018).

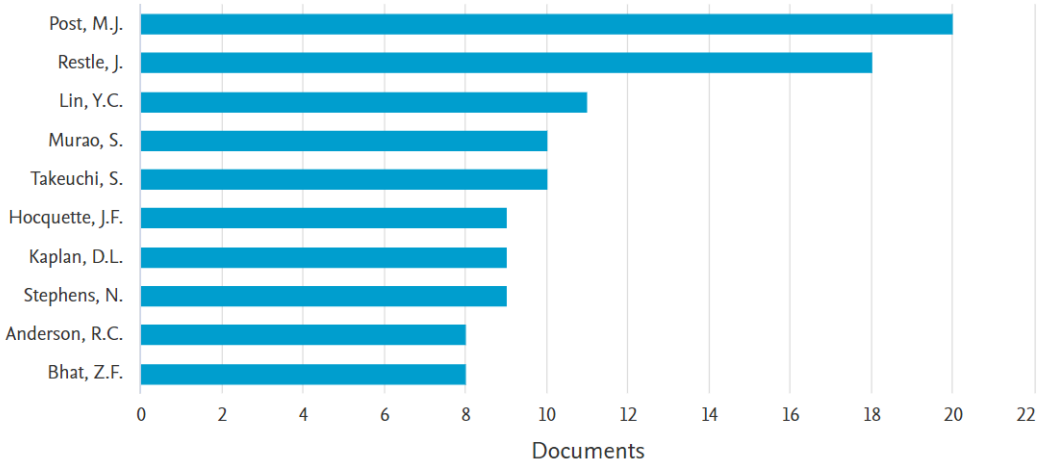

Appendix 5: Number of publications by author in the first iteration (Source: Scopus.com)

Appendix 6: Algorithm for the Image Analysis (Example of the Alg+Gel bioink).

```
close all
clear
clc

myFolder=append(cd,'\Alg+Gel\');

filePattern = fullfile(myFolder,'*.png');
pngFiles = natsortfiles(dir(filePattern));

for i = 1:length(pngFiles)
  baseFileName = pngFiles(i).name;
  fullFileName = fullfile(myFolder, baseFileName);
  ImageArray{i} = imread(fullFileName);
  imshow(ImageArray{i});
  drawnow;
end

%% Coordinates definition

Reading=50;

x1=400;
y1=170;

SquareEnlarging=40;

h=210;

x2=x1-SquareEnlarging;
y2=y1+h-SquareEnlarging;
x3=x1-SquareEnlarging;
y3=y1+2*h-SquareEnlarging;
x4=x1-SquareEnlarging;
y4=y1+3*h-SquareEnlarging;

w=220+2*SquareEnlarging;
h=210+2*SquareEnlarging;

imshow(ImageArray{Reading});
hold on;
rectangle('Position',[x1-SquareEnlarging y1-SquareEnlarging w h],'Edgecolor',
'y');
hold on;
rectangle('Position',[x2 y2 w h],'Edgecolor', 'y');
hold on;
rectangle('Position',[x3 y3 w h],'Edgecolor', 'y');
hold on;
rectangle('Position',[x4 y4 w h],'Edgecolor', 'y');
hold on;
```

```
rectangle('Position',[xFD yFD wFD hFD],'Edgecolor', 'r');


%% Image Analysis

ConvFact=67;  %Conversion Factor from px to mm of the image [px/mm]

for i=1:length(ImageArray)

    eq=histeq(ImageArray{i});

    % Coordinates for Pore Index

    x1=400;
    y1=170;

    SquareEnlarging=40;

    h=210;

    x2=x1-SquareEnlarging;
    y2=y1+h-SquareEnlarging;
    x3=x1-SquareEnlarging;
    y3=y1+2*h-SquareEnlarging;
    x4=x1-SquareEnlarging;
    y4=y1+3*h-SquareEnlarging;

    w=220+2*SquareEnlarging;
    h=210+2*SquareEnlarging;

    %Image cropping

    PR1=imcrop(eq, [x1-SquareEnlarging y1-SquareEnlarging w h]);
    PR2=imcrop(eq, [x2 y2 w h]);
    PR3=imcrop(eq, [x3 y3 w h]);
    PR4=imcrop(eq, [x4 y4 w h]);
    Pore={PR1 PR2 PR3 PR4};


    %Tolerance region growing function

    RegionGRTollerance=0.18;

    %Image plot with cropped regions

    subplot(4,6,[7:8 13:14]);
    imshow(eq);
    hold on;
    rectangle('Position',[x1-SquareEnlarging y1-SquareEnlarging w
h],'Edgecolor','y');
    hold on;
    rectangle('Position',[x2 y2 w h],'Edgecolor', 'y');
    hold on;
    rectangle('Position',[x3 y3 w h],'Edgecolor', 'y');
    hold on;
    rectangle('Position',[x4 y4 w h],'Edgecolor', 'y');
```

```
    hold on;
    rectangle('Position',[xFD yFD wFD hFD],'Edgecolor', 'r');

    %Printability Index calculation

    for k=0:3

        PR=Pore{k+1};
        R=PR(:,:,1);
        G=PR(:,:,2);
        B=PR(:,:,3);
        GM=G>160;
        BM=B>180;
        RM=R>170;
        RGBM=GM-(BM+RM);
        GrayPR=rgb2gray(PR);

RegionGrowth=regiongrowing(im2double(GrayPR),w/2,h/2,RegionGRTollerance);
        Reg=RegionGrowth(:,:,1);
        Reg=Reg.*RGBM;
        se=strel('disk',9);
        RegCL=imclose(Reg,se);
        se=strel('disk',10);
        RegOP=imopen(RegCL,se);
        Edg1=edge(RegOP);
        Over=imoverlay(PR,Edg1);
        Area=regionprops(RegOP,'Area');

        if isempty(Area)==1
            Porosity=0;
        else
            Porosity=Area.Area/(170^2);
        end

        subplot(4,6,3+6*k);
        imshow(Over);
        hold on;
        plot(h/2,w/2, 'r+', 'MarkerSize', 30, 'LineWidth', 1);
        title(append("Printability Index = ",num2str(Porosity*100),"%"));

        PoreInd(k+1)=Porosity;

    end

    set(gcf, 'Units', 'Normalized', 'OuterPosition', [0 0 1 1]);

    PhotoInfo(i,1:4)=[PoreInd];

    drawnow;

end

filename='Alg+Gel.xlsx';
writematrix(PhotoInfo,filename,'Sheet',1,'Range','A1');
```

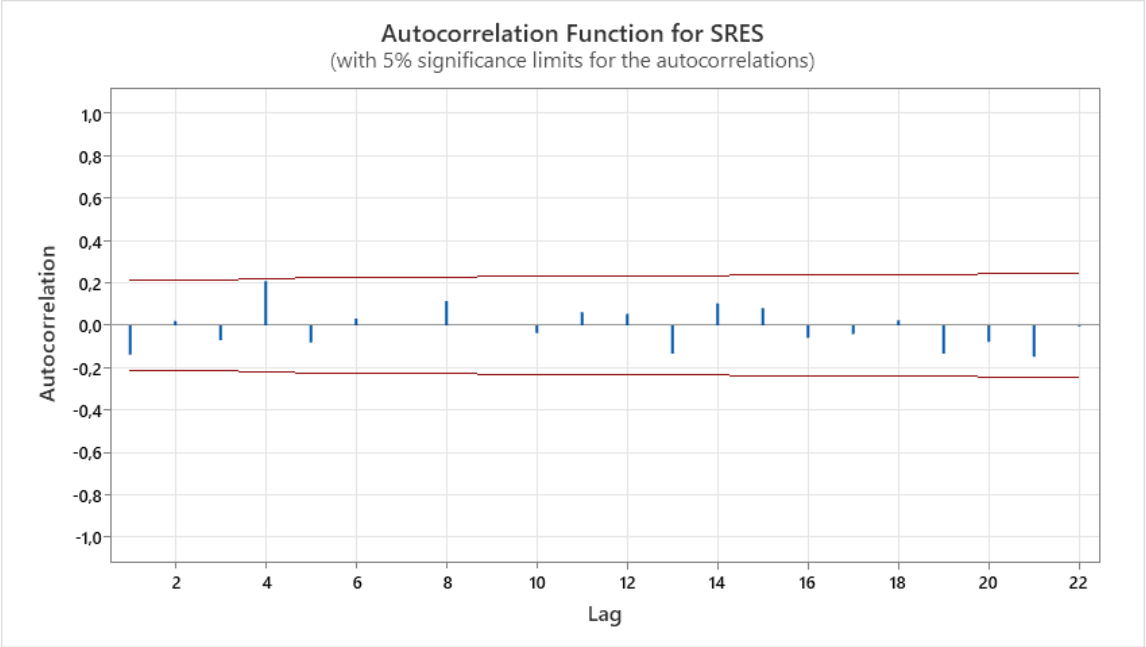

Appendix 7: Autocorrelation Function of the Standardized Residuals of the Alg+Gel model.

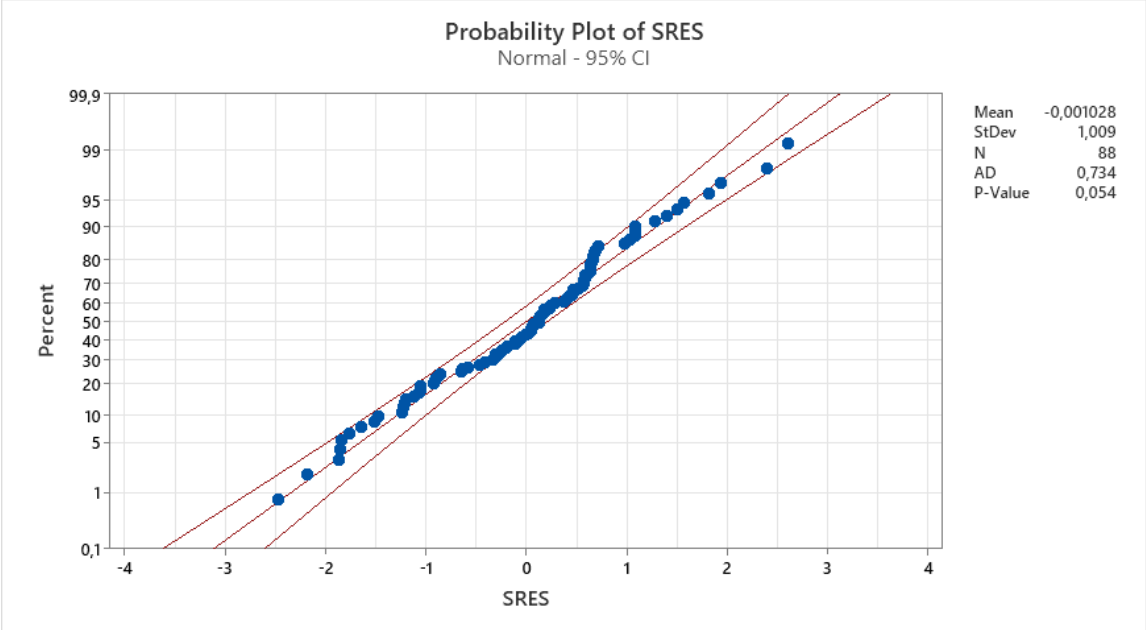

Appendix 8: Normality test of the Standardized Residuals of the Alg+Gel model.

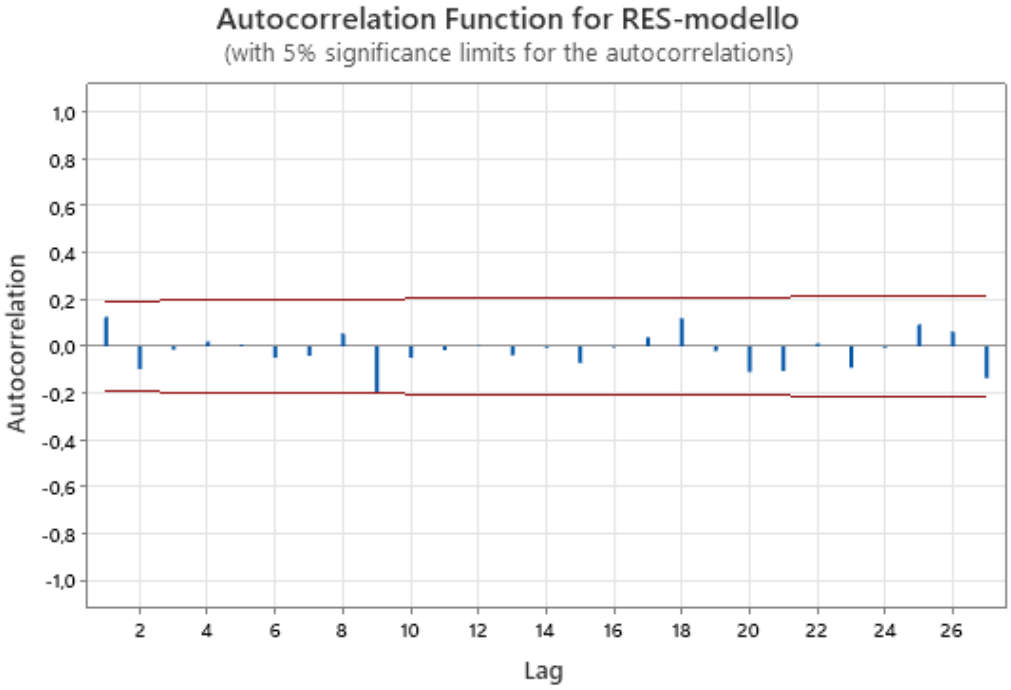

Appendix 9: Autocorrelation Function of the Standardized Residuals of the Alg model.

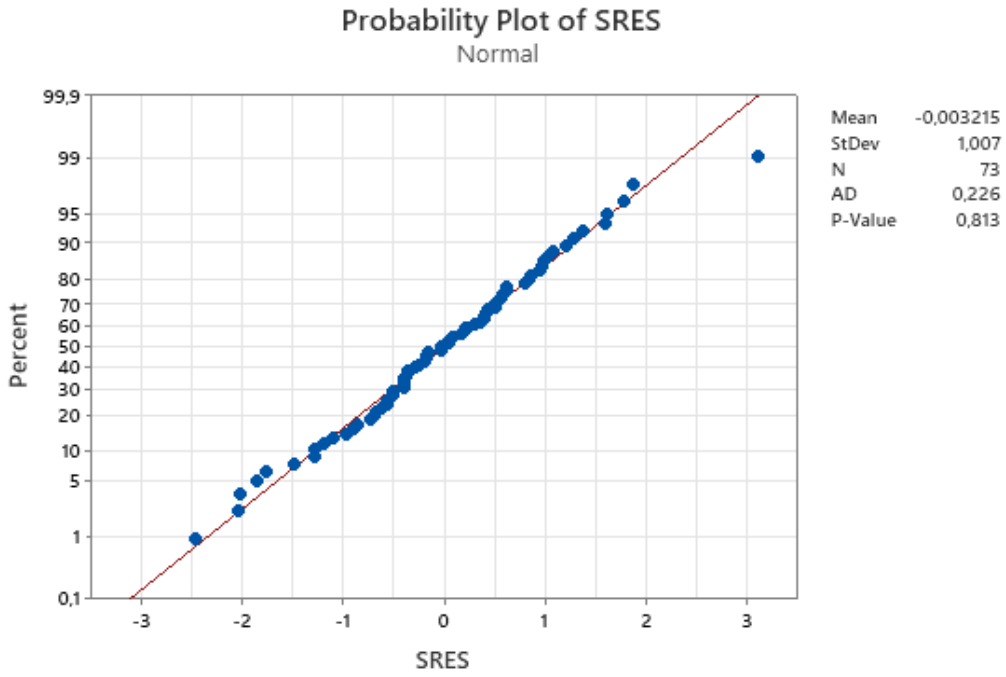

Appendix 10: Normality test of the Standardized Residuals of the Alg model.

List of Figures

List of Tables

List of acronyms

Acronym	Description
CM	Culture Meat
3DBP	Three-dimensional Bioprinting
TE	Tissue Engineering
AM	Additive Manufacturing
SoA	State of Art
DoE	Design of Experiment
FBS	Fetal Bovine Serum
P	Pressure
v	Scanning Speed/Velocity
Alg	Alginate bioink
Alg+Gel	Alginate and Gelatin bioink
UCL	Upper Control Limit
LCL	Lower Control Limit
GHG	Green House Gasses

Acknowledgements

A great thank is extended the advisor Bianca Maria Colosimo, and to Filippo Bracco, the co-advisor of this project who followed me during all the process. An additional thank is to prof. Quirico Semeraro, the colleagues of the *3D cell lab*, and all the people that helped me during this thesis.